RSC Advances

REVIEW

View Article Online
View Journal | View Issue

Advancements in preceramic inorganic polymers for environmental applications: properties, synthesis, and potential uses

Mohammad Mehdi Salehi,†[a] Maryam Mohammadi,†[b] Ali Reza Akbarzadeh,[c] Mohsen Babamoradi,[b] Ali Maleki *[a] and Ehsan Nazarzadeh Zare *[d]

Preceramic inorganic polymers (PCIPs) have garnered attention due to their unique properties and potential applications in environmental contexts. They are highly resistant to heat, making them suitable for high-temperature processes like pollution control, waste management, and water purification. Additionally, PCIPs possess strong mechanical properties, including high strength and stiffness, which enable them to be used in harsh conditions. Their excellent chemical resistance also makes them useful in corrosive environments and as protective coatings for metals. This review explores different methods for synthesizing PCIPs, including sol–gel processing, polymerization, and pyrolysis. Each method has its benefits and challenges, depending on the desired characteristics and intended applications. PCIPs can be utilized in various environmental solutions, including catalytic converters and air filters for pollution

[a]Catalysts and Organic Synthesis Research Laboratory, Department of Chemistry, Iran University of Science and Technology, Tehran 16846-13114, Iran. E-mail: maleki@iust.ac.ir; Fax: +98-21-73021584; Tel: +98-21-73228313

[b]Department of Physics, Iran University of Science and Technology, Tehran 16846-13114, Iran

[c]Department of Chemistry, Iran University of Science and Technology, Tehran, Iran

[d]School of Chemistry, Damghan University, Damghan, 36716-45667, Iran. E-mail: ehsan.nazarzadehzare@gmail.com; e.nazarzadeh@du.ac.ir

† These authors contributed equally to this work.

Mohammad Mehdi Salehi

Mohammad Mehdi Salehi is an emerging research scientist specializing in nanochemistry, with expertise in polymeric nanomaterials. He holds a Bachelor of Science in Applied Chemistry from Zabol University (awarded in 2020 – Guest Student at Shahid Chamran University (SCU) of Ahvaz from Semester 1 to Semester 8) and received his Master of Science in Nanochemistry from the Iran University of Science and Technology (IUST) in 2022, demonstrating a strong commitment to advanced research. Currently a Ph.D. Candidate at IUST, Salehi has advanced his research in polymer-based nanocomposites since commencing doctoral studies in 2023. His work addresses critical challenges through innovative polymer-based nanocomposite development, with core research interests spanning: water purification, environmental engineering, material science, and functional polymeric architectures. His research program pioneers advanced material platforms to address pressing environmental demands.

Maryam Mohammadi

Maryam Mohammadi is a Ph.D. candidate in the Department of Physics at the Iran University of Science and Technology, Iran, working under the supervision of Dr Mohsen Babamoradi. She obtained her B.Sc. in Condensed Matter Physics from Payame Noor University, Qom, in 2013, and her M.Sc. in the same field from the University of Kashan, Isfahan, Iran in 2017. Her research interests lie in the synthesis and application of metal oxide materials and oxide-based nanocomposites for environmental remediation, particularly in the adsorption and degradation of water pollutants.

control, stabilizing hazardous waste, and treating wastewater. They also have potential applications in coatings, composites, and sensors, demonstrating their versatility across various industries. This review offers a comprehensive discussion of PCIPs, concentrating on their properties, production methods, and environmental applications. It also examines future opportunities for utilizing PCIPs in sustainable environmental solutions, emphasizing their crucial role in addressing environmental challenges.

1. Introduction

The interface between polymers and ceramics is critical in materials science. Ceramics can be conceptualized as polymer systems with extensive crosslinking, where the three-dimensional structure imparts strength, rigidity, and thermal resistance.[1,2] While often overlooked, certain ceramics are entirely organic, specifically those based on carbon.[3] Notable examples include melamine–formaldehyde resins, phenol–formaldehyde materials, and carbon fibres.[4–6] Inorganic ceramics, particularly those composed of elements such as

Ali Reza Akbarzadeh

Dr Ali Reza Akbarzadeh is an Assistant Professor in the department of chemistry at Iran University of Science and Technology (IUST). He obtained his Ph.D. in inorganic chemistry (2017) from the IUST, Iran. He spent two years as a Director of Industry Relations, Director of the computer site, and responsible for the Central Computing Laboratory of the Faculty of Chemistry at IUST. He has also been a member of the university's green strategic council. His research interests include combustion synthesis of nanomaterials, elimination of environmental pollutants/absorption, phthalocyanines, catalysts, photocatalysts, and chemometrics.

Mohsen Babamoradi

Dr Mohsen Babamoradi is currently an assistant professor at Iran University of Science and Technology (IUST). He received his Ph.D. from Sharif University of Technology. His research interests include the fabrication and characterization of nanomaterials and nanoscale coatings, thin film applications and surface physics, synthesis and characterization of magnetic nanocomposites, fabrication and characterization of photocatalysts, environmental pollutant adsorbents, and microwave absorption.

Ali Maleki

Prof. Dr Ali Maleki was born in Mianeh, East Azerbaijan, in 1980. He received his Ph.D. in Chemistry in 2009. He started his career as an Assistant Professor at the Iran University of Science and Technology (IUST) in 2010, where he is currently a Full Professor. His research interests focus on the design and development of novel catalysts, nanomaterials, and green chemistry. He has hundreds of ISI-JCR publications. Some of his honors include being named the Distinguished Researcher of IUST from 2010 to 2023, the IUPAC Prize for Green Chemistry in 2016, and being recognized as one of the Top 1% International Scientists in ESI (Web of Science) in 2018, 2019, 2020, 2021, 2022, and 2023.

Ehsan Nazarzadeh Zare

Dr Ehsan Nazarzadeh Zare is an Associate Professor of Polymer Chemistry at Damghan University, Iran. He holds editorial roles at several prestigious journals, including serving as an Editorial Board Member for Inorganic Chemistry Communications and the Journal of Ionic Liquids, and as an Associate Editor for Frontiers in Materials. With over 215 peer-reviewed research and review articles published in high-impact journals, along with three books by ACS and RSC publishers, Dr Nazarzadeh Zare has established himself as a leading researcher in his field. His scholarly impact is further underscored by his consistent inclusion in Stanford University's annual list of the world's top 2% most-cited scientists from 2019 to 2023. His research focuses on the design of advanced biomaterials and functional polymers for applications in environmental remediation, healthcare, and biomedical engineering.

silicon (Si), aluminium (Al), or boron (B) in conjunction with oxygen (O), carbon (C), or nitrogen (N), are widely recognized.[7] Within the realm of inorganic ceramics, two primary categories can be identified: oxide ceramics and non-oxide materials. Oxide ceramics often feature silicate structures characterized by their relatively low melting points. Conversely, non-oxide ceramics, including silicon carbide (SiC), silicon nitride (Si_3N_4), aluminum nitride (AIN), and boron nitride (BN), represent some of the highest melting point materials known.[8–11] Non-oxide ceramics typically possess such high melting points that they present challenges in shaping and fabricating through conventional melt- or powder-fusion methods, which are often used for oxide materials. More than thirty years ago, polymer-derived ceramics (PDCs) were developed by introducing PCIPs, which serve as precursors for manufacturing predominantly silicon-based advanced ceramics.[12] The concept of employing molecular precursors to fabricate ceramic materials was initially proposed by Ainger and Herbert in 1960.[13] In the early 1970s, Verbeek introduced the pyrolysis of organosilicon polymers to produce ceramic materials suitable for high-temperature applications.[14] This technique was specifically designed to produce Si_3N_4/SiC ceramic fibers. The research undertaken by Yajima *et al.* in 1975 on producing SiC fibres from polycarbosilane marked a pivotal advancement in polymer pyrolysis, explicitly targeting the generation of PDCs. Following this basic study, polycarbosilane-derived inorganic polymers (PCIPs), particularly organosilicon polymers, have gained recognition as a highly effective approach for fabricating advanced ceramic materials.[15] It is essential to note that organosilicon polymers are referred to by various terms, including silicon-based polymers, silicon-based preceramic polymers, and silicone resins.[16] The transformation of polymers into ceramics has facilitated remarkable advancements in ceramic science and technology. This method has produced ceramic fibers, coatings, and ceramics that remain stable even at very high temperatures, up to 2000 °C. They also resist breaking down, crystallizing, separating into different phases, and deforming under stress.[17] PCIPs, particularly those formulated as organo-silicon compounds comprising a silicon atom backbone along with C, O, N, B, and hydrogen (H), serve as highly effective means of producing advanced ceramics. Silicon-based polymers containing N, C, and B are used to create different types of non-oxide ceramics, including silicon carbide (SiC), silicon carbonitride (SiCN), and silicon boron carbonitride (SiBCN).[18,19] Ceramic materials have excellent physical, chemical, thermal, mechanical, electrical, magnetic, and optical properties. These properties stem from their strong atomic bonds, which can be either ionic or covalent.[20] These properties make ceramics useful in various industries, including automotive, defense, construction, energy, healthcare, consumer products, and sensor technology.[21] Ceramic materials are grouped into two main types: traditional ceramics and advanced (or technical) ceramics. Traditional ceramics are crafted from natural materials, such as clay and sand. On the other hand, advanced ceramics are generally created through intricate manufacturing processes. Notable examples are SiC, Si_3N_4, BN, aluminium oxide (Al_2O_3), zirconium oxide (ZrO_2), and various composites.[22] Furthermore, recent advancements in the analysis of their nanoscale structure have significantly enhanced the understanding of the distinctive and beneficial properties of polycrystalline diamond composites, particularly regarding their exceptionally high creep resistance, chemical durability, and semiconducting characteristics.[23] From a processing perspective, PCIPs have served as reactive binders in the fabrication of technical ceramics. The design of these materials has been optimized to enable the formation of structured pores at the mesoscale level. Their effectiveness in bonding advanced ceramic components has been assessed, and they can be converted into either bulk or macroporous forms. Consequently, researchers have significantly expanded the possible uses of PDCs.[14] Due to their distinctive characteristics and applications, PCIPs hold considerable promise for addressing environmental issues. These organic polymers can transform ceramic materials *via* regulated pyrolysis techniques, creating inorganic, ceramic-like structures. This conversion opens avenues for utilizing preceramic polymers in various environmental applications, such as pollution remediation, water purification, and sustainable energy solutions.[2,12]

In environmental remediation, preceramic polymers serve as a foundation for creating complex ceramic materials designed with specific characteristics that aim to capture and eliminate pollutants from air, water, and soil. These engineered materials can be optimized for elevated surface areas, enhanced chemical reactivity, and superior adsorption capabilities, effectively addressing environmental contaminants, including heavy metals, organic pollutants, and industrial waste.[24] Additionally, preceramic polymers contribute to technologies by facilitating the production of ceramic components that can withstand high temperatures, which are essential for sensor applications.[25,26]

These polymers, for example, are applicable in fabricating ceramic membranes used for gas separation and purification, as well as solid oxide fuel cells and thermal insulation materials designed for energy-efficient applications.[27–29] The study of preceramic polymers within environmental frameworks involves examining their synthesis, processing techniques, and the characteristics of the resulting ceramic materials relevant to ecological applications. Researchers are focused on advancing novel polymer chemistries and processing methodologies to enhance the efficacy of ceramic materials in environmental remediation and sustainable energy solutions.

In summary, preceramic polymers present significant potential for enhancing environmental sustainability by providing novel approaches to pollution management, water treatment, and clean energy generation. Their distinctive capacity to be transformed into functional ceramic materials underscores their ability to address pressing environmental issues and promote the development of environmentally friendly technologies. Recent studies have focused on applying ceramics to develop novel approaches for environmental remediation. Ceramics play a crucial role in various environmental applications, including detecting, observing, and measuring pollutants, as well as preventing, managing, and remedying their effects.[30] Preceramic polymer materials,

characterized by their unique properties and versatile applications, have emerged as crucial components in environmental reform. This review has examined the studies on PDCs, their synthesis, and their diverse ecological applications. Readers are expected to develop a deeper understanding and appreciation of this field, which they can subsequently apply in their research endeavours.

2. Preceramic polymers

Preceramic polymers, including those containing Si, Al, and B, can lead to a diverse array of compositions in PDCs. Prominent examples of these preceramic polymers typically feature a silicon backbone composed of C, O, N, B, and H elements. Notable types include polysilazanes, polysiloxanes, and polycarbosilanes.[31–33]

Fig. 1a–d illustrates the prevalent silicon-based polymers. Through pyrolysis, silicon-based preceramic polymers can be transformed into various ceramic materials, including silicon oxide (SiO_2), SiC, silicon oxycarbide (SiOC), and SiCN. In contrast to traditional ceramic powders, preceramic polymers provide significantly greater flexibility in fabricating ceramic components characterized by intricate geometric configurations and forms. This technology facilitates the production of a diverse array of high-performance non-oxide ceramics that cannot be produced using traditional ceramic manufacturing techniques. Modifying the chemistry of preceramic polymers, along with the size and morphology of nanofillers, can facilitate the application of nanocomposites (NCs) in intricate shapes and coatings, leading to enhanced thermal and mechanical properties. This versatility is achieved through a range of manufacturing techniques, including casting, moulding, and additive manufacturing (AM).[2,34,35]

PDC technology presents considerable benefits over traditional powder-based ceramic processing and shaping methods, as follows: (1) it can operate entirely as a liquid-based process, thereby circumventing the issues linked to the use of ceramic powders, (2) it provides enhanced formability through the use of soluble and crosslinkable precursors, (3) it facilitates the flexible adjustment of microstructures and compositions at the molecular scale, leading to the development of new capabilities, and (4) the transformation from polymer to ceramic occurs at comparatively lower temperatures (800–1200 °C) than those required in conventional ceramic processing. These benefits have led to PCPs being regarded as exceptionally suitable materials for AM processes, and the integration of AM with PDC technologies has paved the way for potential solutions to the challenges encountered in the synthesis and production of traditional ceramics.[12]

Preceramic polymers exhibit a variety of configurations and microstructures that can influence the microstructure, composition, porosity, and characteristics of the resulting ceramics. Notable silicon-based preceramic polymers, including polysilazanes, polysiloxanes, polycarbosilanes, and polyborosilazanes, are utilized in the production of ceramic materials (Fig. 1a–d).[36–39]

2.1 Si-based preceramic polymers

A general formula has been established for an organosilicon polymer that serves as a precursor in ceramic synthesis. This formula is defined by two essential parameters that affect the alteration and formulation of the preceramic composition at the molecular scale. The first parameter is the group (X) present in the polymer core structure, while the second comprises the substituents R^1 and R^2 bonded to silicon. Changes in the (X) group lead to the development of various categories of silicon-

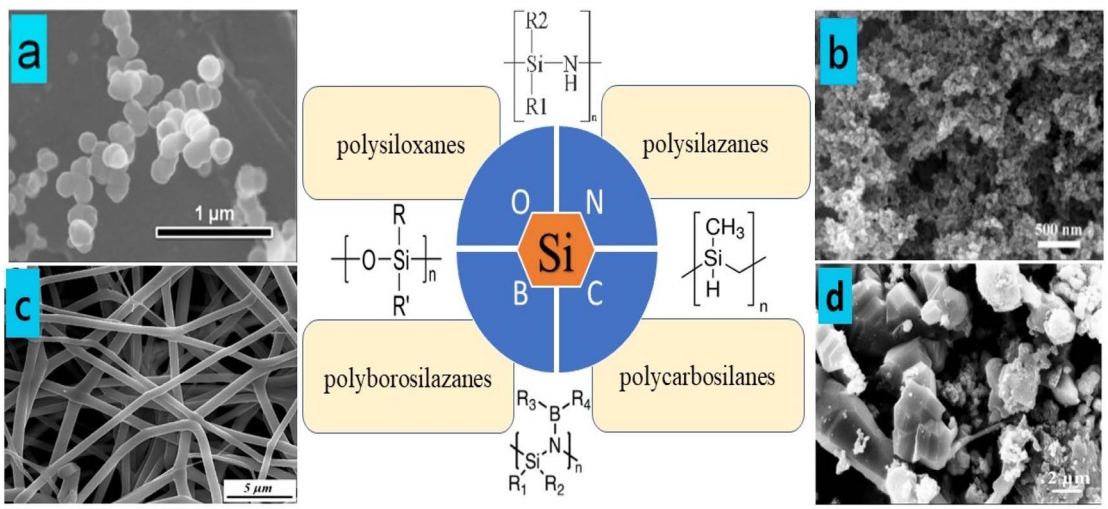

Fig. 1 Common silicon-based polymers: (a) formation of spherical silicon-based nanostructures from polysiloxane using the CVD process. Figure (a) was adapted by permission from: *Surface and Coatings Technology*, 2024, **484**, 130804.[36] (b) SEM images of SiCN aerogels. Figure (b) was adapted by permission from: *Journal of Advanced Ceramics*, 2021, **10**, 1140–1151.[37] (c) SEM image of SiBCN nanofibers after pyrolysis at 1000 °C. Figure (c) was adapted by permission from: *Ceramics International*, 2021, **47**(8), 10958–10964.[38] (d) SEM images showing the structure of β-SiC powders. Figure (d) was adapted by permission from: *Ceramics International*, 2021, **47**(12), 17502–17509.[39]

based polymers. These materials comprise multiple types of silicon-based polymers, characterized by the element or group (X) present in their structure. When X is Si, they are referred to as poly(organosilanes). If X is a methylene group (CH_2), they are known as poly(organo-carbosilanes). When X is O, they are referred to as poly(organosiloxanes). If X is N and H, they are called poly(organosilazanes). Finally, when X is a carbodiimide group ([N=C=N]), they are known as poly(organosilylcarbodiimides).[14]

SiC finds applications in the production of semiconductors, the generation of nuclear energy, and various other industries. Likewise, SiOC, a non-crystalline ceramic produced from polymer precursors, presents a range of applications in both medical and environmental fields.[40,41] Developing composite particles comprising SiC and SiOC represents a promising approach to enhancing material performance. The production of SiOC/SiC ceramics using the polymer-derived ceramics (PDC) method depends on the heat treatment (pyrolysis) of organo-modified polysiloxanes $-[Si(R_2)-O]_n-$ or polysilanes containing oxygen-based functional groups $-[Si(OR_3)]_n-$.[42,43] Silicon, recognized as an excellent precursor for silicon carbide (SiC), is further enhanced by the promising capabilities of polysiloxane as a polymer precursor for silicon oxycarbide (SiOC).

Guo *et al.* utilized organosilane slurry residue (OSR), an organic–inorganic hybrid due to its silicon and polysiloxane components, to synthesize SiOC/SiC. OSR is a byproduct that is a liquid–solid mixture generated within the organosilane manufacturing industries, often regarded as waste. Integrating such waste materials into the synthesis of Stabler NCs presents economic and environmental benefits. The researchers concentrated on the pyrolysis of OSR as a method for synthesizing SiC/SiOC nanocomposites. They aimed to gain an in-depth understanding of the transformation mechanisms, phase transitions, and structural modifications that occur throughout the pyrolysis process.[44]

2.1.1 Organosilicon polymers. The key step in producing silicon-based ceramics is the synthesis of organosilicon polymers, which significantly influences the properties of these materials. Organosilicon polymers are formed by attaching various elements, such as Si, C, O, and N, to the silicon atoms in their core structure. This creates multiple types of polymers, including polysilane, polysilazane, polysiloxane, and polycarbosilane. The chemical groups attached to the silicon atoms, along with the overall molecular structure, significantly impact the properties of the final ceramic, including the ceramic yield and the phase composition of the resulting ceramic, particularly for materials such as SiC, SiOC, and SiCN, as well as the breakdown during processing.[16,45] The chemical structure of the preceramic polymer has a substantial impact on the ceramic yield and the final ceramic structure. The presence of specific functional groups, such as vinyl or methyl, affects both the crosslinking behavior and the amount of carbon retained during pyrolysis. The nature of the organic ligands attached to the Si atoms determines the solubility, volatility, and crosslinking behavior, and ultimately the ceramic yield and microstructure. The backbone structure of the polymer, including the configuration of Si–C or Si–O bonds, along with the presence of side-chain groups (such as methyl or vinyl), plays a crucial role in determining the crosslinking density and thermal stability during pyrolysis. Increased crosslinking, promoted by functional groups such as vinyl groups, improves the ceramic yield by minimizing volatile loss during the transition from organic to inorganic at approximately 1000 °C. For example, vinyl groups facilitate additional crosslinking reactions, thereby enhancing the retention of silicon and carbon in the resultant ceramic.[46,47] Table 1 illustrates the advantages and disadvantages of the preparation methods for organosilicon polymers.

2.1.2 Polysilane. The molecular weight and the type of side chain groups are essential factors that affect the properties of polysilane. The most common way to make polysilanes is through the Wurtz-type coupling of halosilanes. This method involves reacting chlorosilanes with sodium or lithium in a solvent that does not boil easily, like toluene, benzene, or tetrahydrofuran, while heating the mixture. Other methods for making polysilanes include anionic polymerization of masked disilenes, anionic ring-opening polymerization, catalytic dehydrogenation of silanes, and the reduction of dichlorosilanes using magnesium with a Lewis acid and lithium chloride. However, these alternative methods often face problems with instability when exposed to light or moisture, making it hard to control the synthesis of polysilanes.[54]

2.1.3 Polycarbosilane. Polycarbosilanes have complex structures because their core can have different types of carbon chains, such as methylene, vinylidene, and phenylene.[54] Some types of polycarbosilanes have a repeating pattern of π-conjugated units.[55] Polycarbosilane can be synthesized through various techniques, with the Kumada rearrangement of polysilanes being the most prevalent method, applicable under both high-pressure and atmospheric-pressure conditions. Other ways to make polycarbosilanes include the dehydrocoupling reaction with trimethyl silane, ring-opening polymerization, hydrosilylation, and the Grignard coupling reaction, which involves (chloromethyl)triethoxysilane and vinyl-magnesium bromide.[56–58]

To date, polycarbosilane has found extensive applications in the fields of electrical and photoconductive materials, photoresists, and nonlinear optical substances, in addition to serving as preceramic precursors for the production of SiC fibers, powders, whiskers, composites, and nanomaterials. To explore the relationships and distinctions between polycarbosilane and polysilane in the context of SiC ceramics fabrication, Shukla *et al.* conducted a comparative analysis of the thermal properties of various polysilanes and polycarbosilanes. Their research indicated that poly-dimethyl-silane (PDMS) and poly-dimethyl-methyl-phenyl-silane (PDMMPS) are suitable for the synthesis of polycarbosilane through the Kumada rearrangement process.[59] Poly-dimethyl-methyl-silane (PDMMS) has the potential to generate SiC directly, bypassing the need for polycarbosilane synthesis, owing to its significant crosslinking capacity during thermal processing. In contrast, for polycarbosilanes, an increase in molecular weight is correlated with a higher carbon yield, which plays a crucial role in determining the quality of SiC ceramics.

Table 1 Advantages and disadvantages of methods for preparing organosilicon polymers

Methods	Advantages	Disadvantages	Ref.
Sol–gel processes	• Fine control over polymer architecture	• It may exhibit a prolonged duration owing to the incremental characteristics of hydrolysis and condensation, particularly when creating structures with significant crosslinking	48
	• Yield high-purity products	• Excessive water or uncontrolled moisture levels can lead to undesirable side reactions, which may cause the polymer network to become overly	
	• Non-toxic alkoxysilanes, mild conditions such as relatively low temperatures and pressures, and reduced hazardous byproducts	• Post-synthesis treatment: frequently, the produced material necessitates additional curing or ageing processes to attain the intended mechanical characteristics	
Anionic ring-opening polymerization	• This technique yields polysiloxanes characterized by elevated molecular weights, resulting in enhanced mechanical properties, including improved elasticity and toughness	• The anionic polymerization process exhibits a significant sensitivity to impurities, such as water and oxygen, which can potentially halt the polymerization reaction prematurely	49
	• This method enables the precise regulation of polymer chain length and architecture, yielding polymers with	• Demands the use of pure functional monomers—resulting in increased costs and complexity. The high expense of reagents and the necessity for purity require a specialized environment	
	• Functionalized monomers facilitate modifications after the polymerization process		
Grignard reaction	• The method facilitates the incorporation of diverse organic functional groups, such as alkyl and aryl, into the polymer structure, thereby allowing for precise modification of the polymer's chemical and physical properties	• Grignard reagents exhibit a high degree of sensitivity to moisture, which can lead to undesired side reactions and reduced yields	50
	• The procedure exhibits significant reactivity, frequently resulting in the swift synthesis of the intended organosilicon compound	• The reaction frequently produces byproducts, including magnesium salts, necessitating meticulous removal and disposal procedures	
Hydrosilylation	• It typically takes place under mild conditions characterized by moderate temperature and pressure. This approach effectively reduces the likelihood of side reactions and the degradation of sensitive functional groups	• Platinum catalysts are costly, resulting in increased total expenses associated with polymer synthesis, particularly in large-scale industrial applications	51
	• The process of selective bond formation exhibits a high degree of specificity, facilitating the establishment of particular Si–C linkages. This characteristic is advantageous for the synthesis of tailor-made organosilicon polymers	• Hydrosilylation reactions may be adversely affected by specific impurities, such as sulfur, phosphorus, or amines, which can introduce complications in the synthesis process if not meticulously managed	
	• This process produces minimal byproducts, rendering it an effective and environmentally friendly synthesis pathway		
Condensation polymerization	• The condensation polymerization of chlorosilanes exhibits high efficiency and can be readily scaled for industrial manufacturing	• The reaction produces hydrochloric acid (HCl) as a byproduct, necessitating meticulous management and disposal to prevent corrosion and mitigate environmental risks	52
	• Selecting various chlorosilanes, such as those substituted with methyl, phenyl, or vinyl groups, allows for the customization of the resultant polymer's characteristics, including its flexibility and thermal resistance	• Controlling the extent of crosslinking in polymers can be challenging, particularly in systems with high reactivity, which may result in brittle materials	
Polycondensation of silanols	• The procedure is uncomplicated, typically necessitating gentle conditions and yielding the intended polymer without the formation of intricate byproducts	• The condensation reaction may proceed sluggishly, particularly in systems characterized by low reactivity, requiring prolonged reaction durations	53
	• The reaction yields water as the sole byproduct, thereby contributing to the high purity of the resulting polymers	• Attaining an exact level of crosslinking can pose challenges, resulting in variability in the mechanical properties of the final polymer	

2.1.4 Polysilazane. Polysilazanes, characterized by their core structures of alternating Si–N bonds and C-based side groups, serve as essential precursors in the production of SiCN ceramics.[60] Preferential production of Si–N bonds during deposition is due to the greater bonding affinity of Si–N compared to Si–C, as demonstrated by *ab initio* calculations and experimental investigations of a-SiCN films. Because Si–N configurations are more stable (0.52–0.65 eV lower total energy) and have shorter bond lengths, they completely inhibit the production of Si–C bonds regardless of the carbon level. This leads to their domination.[61]

Because of its exceptional thermal stability (≤400 °C), resistance to oxidation, and corrosion protection, polysilazane is used as a heat exchanger barrier and as a coating to protect steel surfaces from environmental deterioration and oxidation.[62] Polysiloxane can be synthesized *via* ammonolysis reactions between chlorosilanes and ammonia or through ammonolysis processes.[63] Another practical approach for synthesizing polysilazane is the ring-opening polymerization of cyclic polysilanane.

2.1.5 Polysiloxane. Polysiloxanes, more often known as silicones, have been around for almost a century and are dependable materials that have many uses in fields such as aircraft, electronics, coatings, and biomedical equipment. The siloxane backbone's unusual flexibility (Si–O–Si) is caused by its broad bond angle (140–180°) and low rotational energy barriers (~2.5 kJ mol^{-1}), which in turn lead to an abnormally low glass transition temperature (*e.g.*, −125 °C for PDMS). Silicones have a lot of great properties, such being very resistant to ozone and UV radiation, having a low surface tension, and being very gas permeable.[64] Polysiloxane can be made using two primary methods: ring-opening polymerization of cyclic silaethers or polycondensation of linear silanes with reactive functional groups. Dimethyl-dichlorosilane is frequently employed in the industrial production of polysiloxanes. Typically, crosslinked polysiloxane demonstrates an enhanced ceramic yield.[14] The sol–gel method utilizes hydrolysis and condensation of hybrid silicon alkoxides to create highly crosslinked polysiloxane. This process can be adjusted by modifying curing chain groups that respond to heat or irradiation.[65–67] A metal alkoxide facilitates composition control and incorporates additional elements into the preceramic network. Adding active fillers to polysiloxane can lead to silicate ceramics other than those based on SiOC. When heated to the correct temperature, polysiloxane functions as a silicon source, reacting with active fillers to form the intended ceramic material.[68]

2.1.6 Other organosilicon polymers. Many organosilicon polymers have been developed that go beyond the commonly known ones. One crucial example is polysilylcarbodiimides, which have the formula $-[R_1R_2Si–X]_n-$, where X stands for N=C=N, and the R groups can be hydrogen, phenyl, ethyl, methyl, and others. These compounds are used as starting materials to produce SiCN-based ceramics.[69] Polysilylcarbodiimides can be synthesized through a reaction using pyridine as a catalyst, with chlorosilanes and bis(trimethylsilylcarbodiimide); however, they are sensitive to moisture.[70] In a recent study, researchers identified hyperbranched polycarbosiloxanes as distinct ceramic precursors of SiCO, which improve ceramic yields.[71] Organosilicon polymers containing boron, such as polyborosilane, polyborosilazane, polyborosiloxane, and their derivatives, are frequently precursors in producing borosilicon ceramics. In contrast to conventional organosilicon polymers, incorporating metal elements (such as zirconium and iron) into the main chain or side chains of preceramic polymers facilitates the creation of cermet.[72]

Many studies have demonstrated progress in developing affordable and straightforward methods for producing functional organosilicon polymers with high ceramic yields. These studies also explored how the structure of the polymers affects the properties of the ceramics made from them. It is essential to note that the final properties of the ceramics depend significantly on the subsequent processes, such as shaping, crosslinking, and sintering.

3. Properties of preceramic inorganic polymers

Polymers of both organic and inorganic composition differ primarily in their backbone composition; organic polymers contain C atoms, while inorganic polymers lack carbon atoms in their structure and incorporate Si, phosphorus, and N instead. The structural forms of organic polymers are typically more straightforward than those of inorganic polymers, which tend to be more intricate and highly branched.[73] It is also possible for hybrid polymers to contain both organic and inorganic segments within the same polymer backbone. Other characteristics of polymers made from mineral materials include their unique properties, which are not found in organic materials, such as flexibility at low temperatures, conductivity, and flame resistance. Unlike silicate minerals, which are extensively crosslinked, inorganic polymers are typically one-dimensional. This section will elucidate several of these characteristics.[74]

3.1 Thermal stability

Preceramic polymers demonstrate essential thermal stability for high-temperature applications and ceramic conversion, maintaining structural integrity during pyrolysis. This property enables their use in aerospace components, thermal protection systems, and high-temperature coatings where decomposition resistance is critical.[56] Several factors affect the thermal stability of preceramic inorganic polymers, including:

(I) Chemical composition: the type of inorganic elements and their bonding in the polymer play a key role. Ceramic precursors with more robust, thermally stable bonds exhibit better thermal stability.[75]

(II) Polymer structure: the configuration of atoms within the polymer chain significantly influences its thermal properties. Typically, polymers with well-defined and organized structures exhibit better thermal stability than those with disordered arrangements.

(III) Crosslinking density: increased crosslinking within the polymer framework can improve thermal stability. Crosslinked networks exhibit a reduced susceptibility to degradation when subjected to high temperatures.

(IV) Presence of volatile components: certain preceramic polymers may possess volatile constituents that can be emitted at elevated temperatures, thereby influencing the overall stability of the material.

(V) Pyrolysis conditions: the thermal stability of the preceramic polymer can be influenced by the specific conditions of pyrolysis or heat treatment, including temperature, duration, and atmospheric environment.

Researchers and materials scientists investigate and enhance these variables to create preceramic inorganic polymers that exhibit superior thermal stability. The objective is to formulate materials capable of withstanding the necessary processing temperatures throughout the conversion to ceramics while preserving the desired characteristics.[76,77] The thermal characteristics of PDCs play a crucial role in their utilization in high-temperature applications, such as heat-protective coatings and insulating materials. The main thermal factors related to PDCs include thermal conductivity (κ), electrical conductivity (σ), coefficient of thermal expansion (CTE), specific heat capacity (C_p), thermal diffusion rate (α), and thermal shock resistance (TSR). Among these, thermal conductivity is the most critical factor, and this discussion will focus mainly on it.[78]

The transition of phonons primarily governs the κ of ceramic substrates characterized by robust covalent bonds. The microstructural features of these materials, including impurities, crystallinity, grain boundaries, microcracks, and micropores, have a significant impact on phonon scattering, thereby influencing the thermal properties of the materials. Subsequently, we will discuss how the microstructure of PDCs affects their thermal efficiency. Both crystallinity and impurities significantly influence the thermal characteristics of a PDC. The impurities can be categorized into two components: the first pertains to the phase produced by PDCs within the heat treatment process, primarily referring to free carbon.

In contrast, the second involves intentionally adding dopants to modify thermal characteristics. Free carbon has varied effects on PDCs depending on the system in which it appears. In the case of the PDCs–SiOC composite, the presence of free carbon markedly enhances the κ of SiOC. For instance, incorporating cost-effective, readily available carbon-based fillers such as lamp black (LB), graphite (GR), carbon black (CB), and activated carbon (AC) into a SiOC system was successfully achieved through abrasion milling, then spark plasma sintering, resulting in dense, bulk composites without crack. The carbon-enriched SiOC systems (C–SiOC) exhibited improved κ (Fig. 2a). The SiOC performed 63% better when GR flakes were integrated than when standard SiOCs were used. Furthermore, CB did not exhibit a 46% increase in κ due to phonon and electron transfer efficiency, as it created a permeating network of highly interconnected and tortuous carbon domains within a graphene-like structure. The amorphous SiOC exhibits a notably low intrinsic κ, measured at $\sim$1.2 W (m K)$^{-1}$ at ambient temperature. Consequently, free carbon significantly enhances the κ within the PDCs–SiOC system.[79]

Defects, including micropores, microcracks, grain boundaries, impurities, and variations in crystallinity, significantly influence the thermal characteristics of polycrystalline diamond composites. The effect of these defects on thermal characteristics primarily occurs through their impact on phonon scattering. The presence of small pores, cracks, and grain boundaries can increase the scattering of phonons, which reduces thermal conductivity. Pang *et al.* calculated the κ of heavily N-doped and B-doped cubic SiC by considering how phonons scatter with electrons and defects. Their analysis revealed that in the case of N-doping, both types of scattering contribute to reducing thermal conductivity. Specifically, phonon–electron (ph–el) scattering primarily contributes to the decrease in κ when defect concentrations are below approximately 10^{20} cm^{-3} at room temperature. However, phonon–defect ph–def scattering becomes the prevailing mechanism as the doping concentration exceeds this threshold.

In contrast, for B-doping, ph–def scattering mainly reduces κ across all the temperatures and doping levels tested (Fig. 2b). The study also looked at how κ changes with temperature for two different defect concentrations, $C_{def} = 10^{19}$ and 10^{20} cm^{-3}, as shown in Fig. 2c. For N-doping at a concentration of 10^{19} cm^{-3}, the effect of ph–def scattering on reducing κ is small, especially at temperatures higher than room temperature, like at 300 K. This pattern is true for both individual and combined scattering effects in N- and B-doped 3C–SiC. Fig. 2d shows the intrinsic rates of three-phonon, ph–el, and ph–def scattering at room temperature with a concentration of $C_{def} = 10^{20}$ cm^{-3}.

For B-doping, the ionization energy of B defects is about 0.65 eV, which is much higher. This higher energy reduces the ph–el scattering rates, so they can be ignored because the carrier concentration is very low. The focus should be on ph–def scattering from neutral defects, as their scattering rates are similar to three-phonon scattering rates. On the other hand, the ionization energy of the N-defect is much lower, around 0.07 eV. This makes both ph–el and ph–def scattering essential to consider in the low-frequency range, where phonons mainly affect κ, the scattering rates from neutral defects and ph–el interactions are similar to those of three-phonon processes. Therefore, both ph–el and ph–def scattering are expected to reduce significantly κ in highly N-doped 4H–SiC, unlike in B-doped materials.

Because ph–def scattering is not influenced by temperature (T) and intrinsic anharmonic scattering escalates linearly with T, the relative reduction κ diminishes at elevated temperatures. This phenomenon is particularly observable in the case of B dopant. Specifically, ph–def scattering, particularly when B is present, exhibits minimal temperature dependence; consequently, the decline in κ remains consistent even at high temperatures.

In contrast, the increase in ph–el scattering with T is significant in the case of N dopant (N_C), resulting in a more rapid decrease in κ compared to B_C. This results in a lower κ above 400 K for N_C with a concentration of 10^{20} cm^{-3}. These findings underscore the importance of considering the ph–el scattering mechanism alongside other phonon scattering

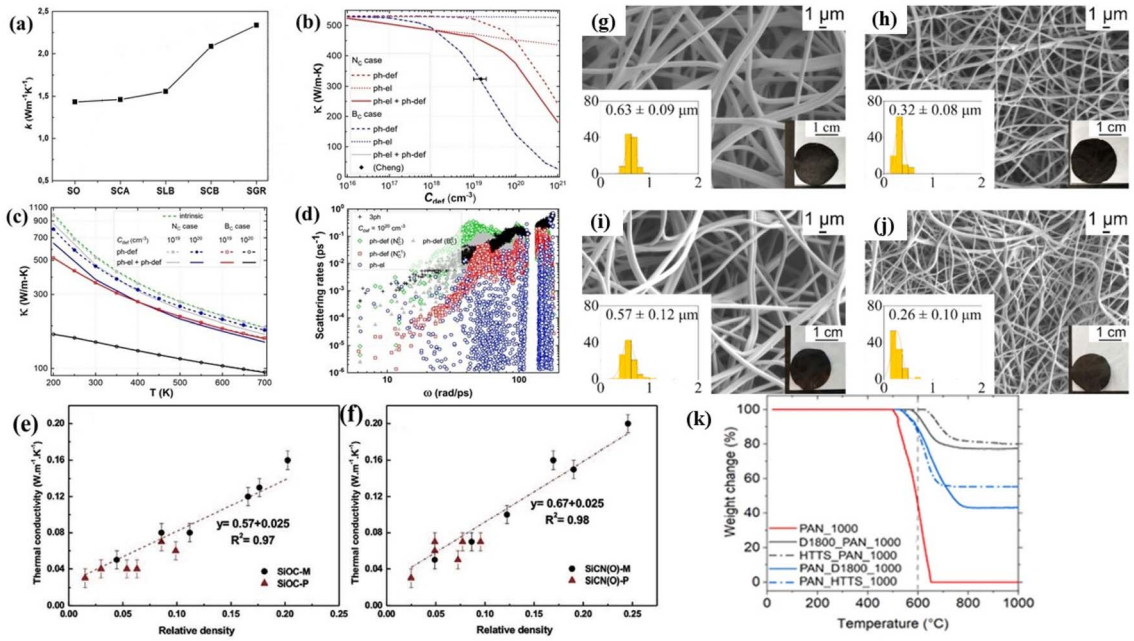

Fig. 2 (a) κ of incorporating GR, LB, CB, and AC into a SiOC matrix named SGR, SLB, SCB, and SCA. Figure (a) was adapted by permission from: *Journal of Alloys and Compounds*, 2021, **889**, 161698.[79] (b) An analysis of the κ reduction at 300 K for the extrinsic N- and B-doped case, focusing on the contributions of ph–el and ph–def scattering mechanisms, both independently and in combination, across a range of defect concentrations from 10^{16} to 10^{21} cm^{-3}. (c) The temperature dependence of κ within the range of 200 to 700 K for both nitrogen-doped and boron-doped cases is characterized by defect concentrations of 10^{19} and 10^{20} cm^{-3}. This analysis encompasses ph–def and ph–el scattering mechanisms, considered separately and in conjunction. (d) The ph–def scattering rates for neutral B^0_C, neutral N^0_C, and charged N^{+1}_C defects at a defect concentration (C_{def}) of 10^{20} cm^{-3}, alongside the associated ph–el scattering rates at an electron concentration of 7×10^{18} cm^{-3}. Additionally, the three-ph scattering rates at a temperature of 300 K in 4H–SiC are included. Figures (b)–(d) were adapted by permission from: *Materials Today Physics*, 2024, **41**, 101346.[80] Presents the κ quantities at room temperature for the following materials: (e) SiOC and (f) SiCN(O) ceramic foams. The triangles denote the open cell structures, classified as P-type, while the black circles represent the ceramic foams' closed cell configurations, identified as M-type. (For a detailed understanding of the colour references in this figure legend, readers are encouraged to consult the online version of this article). Figures (e) and (f) were adapted by permission from: *Ceramics International*, 2020, **46**, 5594–5601.[81] SEM images depicting mean fibre diameter, corresponding histograms, and optical images of (g) D1800_PAN_1000, (h) HTTS_PAN_1000, (i) PAN_D1800_1000, and (j) PAN_HTTS_1000, (k) TGA curves of C-rich SiCN(O) and carbon nonwovens for assessing oxidation resistance (heating rate: 5 K min^{-1}; atmosphere: synthetic air). Figures (g)–(k) were adapted by permission from: *Journal of the European Ceramic Society*, 2024, **44**(9), 5308–5318.[82]

processes when assessing the thermal conductivity of doped semiconductors, such as the development of thermal insulators and thermal shields in extreme conditions.[80]

Santhosh *et al.* created foam materials from polymers, specifically SiCN(O) and SiOC, and tested their thermal properties. Their results showed that, within the temperature range of 30–850 °C, the linear thermal expansion coefficients for the SiCN(O) and SiOC foams were 1.72×10^{-6} K^{-1} and 1.93×10^{-6} K^{-1}, respectively. Additionally, both types of foams had very low thermal conductivity at room temperature, with SiCN(O) ranging from 0.03 to 0.2 W (m K)$^{-1}$ and SiOC from 0.03 to 0.6 W (m K)$^{-1}$. These results highlight the critical role of the foam's structure on its thermal properties.[81] To understand how the structure affects thermal conductivity, especially when comparing open-cell and closed-cell foams, the researchers presented data on the relative density of these materials, showing apparent differences between the two types of cells (Fig. 2e and f). The findings in Fig. 2e and f show that P-type and open-cell polyurethane (PU) foams generally have a lower relative density than M-type PU foams. In particular, PU foams with semi-closed cells can accommodate more preceramic polymers, resulting in denser materials after undergoing thermal decomposition.

Nevertheless, despite this significant distinction between the two foam types, the relationship between κ and relative density remains consistent, with all data points for each chemical composition aligning along the same primary trend line. Balestrat *et al.* synthesized amorphous Si–B–C powder using B-modified polycarbosilane and modified its thermal characteristics. Their research indicated that the porosity of the sintered sample diminished considerably as the boron content increased, subsequently enhancing the κ of the material. Polycarbosilanes with 0.7% boron have demonstrated that incorporating boron into SiC powders enables the formation of dense ceramics at temperatures as low as 1750 °C. These ceramics have a Vickers hardness between 9.6 and 17.3 GPa and a thermal conductivity ranging from 17.7 to 45.1 W (m K)$^{-1}$.[83]

3.2 Mechanical properties

The industrial production of SiC-based ceramic fibers is achieved by transforming polycarbosilane, utilizing a method

pioneered by Yajima and colleagues in the 1970s and 1980s.[15] SiC-based ceramic fibers have undergone significant improvements over time. The first generation had too much carbon, high oxygen levels, and an unclear structure. The third generation, however, has a nearly balanced composition and a crystal-like structure. Polycarbosilane is the primary component of Nicalon fibre, which is produced using Nippon Carbon's Yajima process. During the curing of the first generation of Nicalon fibres, oxygen is introduced into the system at temperatures of up to 12 wt%. Si(O)C fibres were more suitable for describing these fibres. High-temperature stability and creep were found to be adversely affected by the presence of oxygen. When oxygen is present in SiOC, it decomposes above 1200 °C, resulting in weight loss, the growth of SiC crystals, and a loss of strength. The strength and elastic modulus of these fibres were found to reach 3 and 200 GPa at room temperature. Curing processes utilizing ion irradiation were developed to reduce oxygen content and enhance high-temperature stability.[84–86] Recent advancements in chemical composition have enabled the development of SiC fibres with properties similar to those of bulk SiC. These fibres are powerful at temperatures up to 1400 °C, an elastic modulus of 400 GPa.[87] In 1976, Yajima and his group attempted to enhance the thermal stability of these fibres by incorporating filler elements such as Al and Ti into the material system. To improve thermal stability, titanium alkoxides were used to modify polycarbosilane, resulting in Si–Ti–C–O fibers with high-temperature resistance.[88] Al-modified SiC fibres have been developed based on a similar concept. A unique feature of the SiAlCO fibres is that they maintain their mechanical integrity at temperatures as high as 1900 °C and display a tensile strength of 2.5 GPa and an elastic modulus of 300 GPa.[89]

3.2.1 Bulk and dense PDCs. The study of PDCs' mechanical properties faces challenges in producing bulk test specimens. Two methodologies are employed: the powder route, which directly pyrolyzes green compacts, and the liquid route, which utilizes sol–gel solutions or polymers for casting, resulting in dense, crack-free monolithic PDCs.[87] Continuous SiOC ceramic fibres were produced using an innovative sol–gel technique incorporating polyethene oxide (PEO). Modifying the viscosity and composition of the solution in which precursor fibres were synthesized was possible. An optimal spinning solution was achieved by carefully combining tetraethylorthosilicate, methyltrimethoxysilane, sucrose, and PEO. Several factors, including pyrolysis temperature and C/Si ratio, were examined in the study to determine how these parameters affected the microstructure and mechanical properties of the ceramic fibres produced from SiOC.[90] Making fully dense SiOC materials from polymer or sol–gel hybrid ceramics is difficult. During pyrolysis, the release of gases causes shrinkage and mass loss, resulting in residual pores and internal stresses within the material. These issues can create defects and cracks in the final product. To achieve dense SiOC materials, several methods have been employed, including the use of fillers, thermal oxidation, hot pressing, pyrolysis, cross-linking, liquid casting with pyrolysis, photo-crosslinking, and traditional techniques. Ceramic processing techniques, including standard firing methods such as uniaxial or isostatic pressing and hot pressing.[91]

Consequently, traditional methods make it challenging to achieve dense PDCs. PDCs cannot be further used due to these issues, which limit their integrity and mechanical strength. Liquid polymer precursor compositions can be adjusted to achieve ceramics with an integrated functional structure, in contrast to traditional ceramic preparation methods. Thus, PDCs must be strengthened mechanically. Research has explored methods to increase PDC density, including optimizing processes, incorporating passive or active fillers, applying pressure, or repeating the impregnation-pyrolysis process. For instance, Hanniet *et al.* used direct photolithography of photocurable B-containing polyceramic polymers with molecular design to create dense, crack-free SiBCN microparticles (20–200 μm) with a Young's modulus of 60 GPa.[92]

3.2.2 Hardness and fracture toughness. The Vickers hardness of silicon carbon oxides (SiOCs) increases with elevated pyrolysis temperatures and carbon incorporation into the amorphous silica matrix. This trend is also observed in materials within the Si–C–N and Si(O)C systems. SiCN and Si(O)C materials have notably higher hardness than SiOCs, with values ranging from 8 to 15 GPa.[14] Volume densification has a significant impact on the deformation process beneath the indenter, resulting in circumferential Hertzian cone fractures. The SiCN system exhibits less pronounced behaviour due to its more interconnected covalent network. In both SiOC and SiCN systems, increasing the pyrolysis temperature promotes dehydrogenation, resulting in a more connected network, which reduces the effect of volume densification and enhances the effects of shear deformation. This alteration in the deformation mechanism leads to a transition from an "anomalous" fracture pattern to a more "normal" one. A substantial increase in the hardness of SiCN materials with rising indentation loads is observed.[93,94]

Additionally, using the pyrolysis approach of polymer crosslinked polysiloxane, Sorarù *et al.* created SiOC glasses in thin, dense, and crack-free samples last year. In this study, the amount of free carbon in the final SiOC materials ranged from 18% to 60%. The nanoindentation technique was used to measure the mechanical properties of SiOC glasses, and both Young's modulus and hardness decreased with increasing free carbon content, following a simple law of the mixture model.[95] For fracture toughness (K_{IC}), SiCN and SiOC PDCs produced through liquid and powder processing methods are evaluated. K_{IC} values range from 0.56 to 3 MPa $m^{1/2}$, with higher values observed in powder-fabricated PDCs due to R-curve behaviour influenced by the specific processing technique.[96,97] K_{IC} values for liquid-produced PDCs are typically lower, with a particular measurement of 0.70 MPa $m^{1/2}$ for a SiOC synthesized from a sol–gel precursor. Full-density SiCN derived from liquid precursors has K_{IC} values ranging from 0.56 to 1.3 MPa $m^{1/2}$.[93,97] Through the integration of multi-phase design, doping, fiber reinforcement, and process control, dense SiC-based PDCs can be engineered to attain elevated levels of fracture toughness, mechanical strength, and thermal resilience, essential attributes for rigorous applications in the aerospace, nuclear, and

energy industries.[98] The incorporation of fillers represents a well-recognized method for enhancing the characteristics of PDCs. For example, Yamamura *et al.* successfully synthesized Ti-doped Si–O–C, achieving thermal stability beyond 1200 °C. In a similar vein, Al was investigated as a filler material, with the resulting Si–Al–C–O fibers demonstrating exceptional thermo-mechanical stability at temperatures exceeding 1900 °C in an inert environment and 1000 °C in air.[89] This indicates that the inclusion of Ti and Al dopants contributes to improvements in both mechanical properties and high-temperature resistance. To further enhance the K_{IC} of PDCs, an attempt was made to incorporate nanofillers into the material. For example, the introduction of 2 mass% CNT resulted in a 60% increase in K_{IC}. This improvement was linked to the toughening mechanisms of fibre bridging and fibre pullout (CNTs function as crack deflectors and toughening agents, thereby significantly improving K_{IC}).[99]

The processing parameters, including thermolysis temperature, significantly influence the outcomes. The Vickers hardness exhibited an increase from 7.9 to 12.8 GPa as the thermolysis temperature rose to 1400 °C; however, it subsequently declined at 1550 °C due to the effects of crystallisation and porosity. Thus, optimizing the pyrolysis temperature is essential for enhancing densification while reducing microstructural defects. The integration of chemical modifications (such as dopants including Ti, Al, and B), physical reinforcements (like CNTs and fibers), and optimization of processing techniques (for instance, SPS, thermolysis control, and additive manufacturing) provides a thorough approach to improving fracture toughness and mechanical strength in SiC-based PDCs while maintaining high-temperature stability.[87]

3.3 Chemical resistance

3.3.1 Oxidation resistance. PDCs were initially designed for applications involving high temperatures, which has led to extensive research on their oxidation resistance. A recent review has summarized findings in this area. PDCs from the Si–C, Si–C–O, Si–C–N, and Si–B–C–N systems have all had their oxidation behaviour carefully studied. Typically, parabolic oxidation rates are noted for PDCs that have been pyrolyzed at sufficiently high temperatures to eliminate all hydrogen from the material.[100–102]

Kovalčíková *et al.* studied how SiC ceramics react to oxidation at temperatures between 1350 and 1450 °C for up to 204 hours. They examined how various processing methods impacted this reaction. The SiC ceramics were produced using a fast-hot-pressing method with granular SiC powder, without the addition of any oxide sintering aids. Compared to traditional techniques, this novel technology enables a reduction in sintering temperature of approximately 200 °C. The SiC produced without additives exhibited superior oxidation resistance compared to SiC that underwent hot pressing with liquid-phase sintering, demonstrating a roughly three orders of magnitude lower parabolic oxidation rate. The newly developed SiC ceramics have impressive properties, including a Vickers hardness greater than 27.4 GPa, a fracture toughness of 3.42 MPa $m^{1/2}$, and excellent oxidation resistance, measured at 4.91×10^{-5} mg^2 $(cm^4\ h)^{-1}$ at 1450 °C.[103] Recent research has yielded new findings regarding the thermodynamic stability of SiC(O) and SCN(O) ceramics, which are produced by heating various polymer precursors (polycarbosilane, polysilazane) at 1200 °C. While the polysilazanes have similar structures, they differ in their crosslinking temperatures. High-resolution X-ray photoelectron spectroscopy reveals significant differences in the microstructure of each material. The enthalpies of formation ($\Delta H^{\circ}_{f,elem}$) for SiC(O) (from polycarbosilane), SCN(O) (from polysilazane), and SCN(O) (from polysilazane) are measured at -20 ± 4.63, -78.55 ± 2.32, and -85.09 ± 2.18 kJ $(mol)^{-1}$, respectively. Among these, the PDC derived from polysilazane exhibits the highest level of thermodynamic stability. The findings indicate that incorporating N into the microstructure of PDCs enhances thermodynamic stabilization. The thermodynamic analysis reveals a greater thermodynamic impetus for forming SiCN(O) microstructures as the proportion of SiN_xC_{4-x} mixed bonds increases while the presence of silica diminishes. Overall, the enthalpies of formation demonstrate that SiN_xC_{4-x} mixed bonds exert a more pronounced stabilizing influence than SiO_xC_{4-x} mixed bonds. The findings imply that a decrease in silicon and oxygen concentration is correlated with a systematic stabilizing of SiCN(O) complexes. Furthermore, the destabilization of PDCs associated with elevated silicon levels may plateau at higher concentrations.[104]

Compared to their crystalline forms, like Si_3N_4, SiC, and graphite, carbon-rich SiCN ceramics made from polysilylcarbodiimides (which do not have mixed bonds) show slightly positive or nearly zero heat changes when tested for oxidative dissolution in a molten oxide solvent.[105] The findings indicate that the enthalpy of formation for PDCs is significantly influenced by the existence of mixed bonding within their atomic framework. Additionally, research has explored the effects of incorporating supplementary elements into SiCN PDCs on their oxidation characteristics.

In the study by Ramlow *et al.*, polyacrylonitrile (PAN) solutions were mixed with different amounts of oligosilazane (Durazane 1800) or polysilazane (HTTS made from Durazane 1800) and electrospun to create C-rich SiCN(O) nonwovens. By adjusting the viscosity of the solutions, they created fine fibers with diameters ranging from 0.32 μm to 0.62 μm. The fibers were then heated to 1000 °C in a N_2 environment, transforming them into amorphous C-rich ceramic nonwovens with various Si–C–N–O phases dispersed throughout the fibers. The diameter of the fibres following pyrolysis at 1000 °C was unexpectedly found to range from 0.26 to 0.63 inches, likely attributable to the fusion of fibres during the process (Fig. 2a–d). Using oligosilazane with PAN resulted in increased oxygen contamination, which enhanced ceramic yields through supplementary crosslinking reactions.

Additionally, all samples exhibited a higher initial oxidation temperature than pure carbon, approximately 500 °C. Materials with a higher content of PAN demonstrated minimal impact on the protective capabilities of the matrix. This is attributed to the limited formation of ceramic phases, which were insufficient to establish a dense passive layer necessary for safeguarding the substantial quantity of free carbon present. Consequently, the

HTTS_PAN_1000 sample, characterized by a high polysilazane content, exhibited the most effective oxidation resistance at temperatures of up to 600 °C (Fig. 2k). The polysilazane helps create a strong protective layer that shields the free carbon areas. As a result, the improved resistance to oxidation of the nonwoven HTTS_PAN_1000 is primarily due to the specific chemical composition and molecular structure of the polymers, which facilitate a uniform distribution of free carbon within the fiber matrix. The study demonstrates that carbon-rich SiCN(O) nonwovens possess significant potential for use as catalyst supports in high-temperature, harsh environments, as well as for lightweight materials due to their low density. It also highlights the advantages of PDC technology, showing that the properties of the resulting ceramics can be easily adjusted by modifying the composition or chemical structure of the polymers.[82]

The role of boron seems to be complex. The initially observed low oxidation rates for Si–B–C–N ceramics may have been underestimated for several reasons, including the small ratio of oxide to ceramic volume, the thick flow of borosilicate, and the evaporation of B_2O_3.[106,107] Studies have shown Kp (or αKp) values similar to those of SiC and Si_3N_4 at a temperature of 1500 °C. When aluminum is added to Si–C–N–(O), it causes the oxidation behavior to change, especially at temperatures above 1000 °C. This results in a quicker decrease in oxidation rates, eventually reaching a low point. At 1400 °C, the oxidation rate becomes stable. It follows a parabolic pattern for over 20 hours, with rate constants approximately ten times lower than those found in Si–C–N samples without aluminum. Aluminum influences the structural evolution of SiAlCN ceramics by stabilizing the $SiCN_3$ structure at high temperatures and thus delays the crystallization of SiAlCN ceramics. Aluminum also enhances the phase transformation of α-Si_3N_4 to β-Si_3N_4 during the crystallization of polymer-derived SiAlCN ceramics. Also, the oxidation rate of SiAlCNs is more than one order of magnitude lower than that of SiCN without aluminum and CVD-derived SiC and Si_3N_4. The reduced oxidation kinetics of SiAlCNs is due to the unique structures of the oxide precipitates formed by SiAlCNs, in which the aluminum atoms are located in 6-membered Si–O rings, preventing the penetration of oxygen. These aluminum-doped ceramics exhibit remarkable resistance to water vapor-related corrosion at high temperatures. Compared to other silicon-based non-oxide ceramics, SiAlCNs have the lowest corrosion rate. Additionally, SiAlCNs have smooth surfaces and retain high strength after heat treatment. This unique property is attributed to the formation of a protective Si–Al–O layer, in which a small amount of aluminum significantly reduces the activity of silica.[108]

3.3.2 Chemical durability. The research by Soraru *et al.* investigated the chemical durability of SiOC glasses with varying levels of "free" carbon in basic or acidic environments. The results show that the SiOC network is more durable than pure silica glass (SiO_2) in both basic and acidic conditions. This improved durability is due to the nature of the bonding, as Si–C bonds are less susceptible to nucleophilic attack. Also, the added disorder and crosslinked carbon in the network—whether attached to silicon atoms or existing as "free" carbon—help block the movement of reactants. When SiOC is heated to high temperatures ($T \geq 1200$ °C), it separates into regions rich in SiO_2, SiC, and carbon. This process lowers the chemical durability because the SiO_2 parts become easier to remove. If SiOC glass is treated with a strong hydrofluoric acid (HF) solution, the SiO_2 phase can be removed entirely.[109]

4. Synthesis of preceramic inorganic polymers

PDCs are ceramics made from polymeric materials, unlike those produced through conventional powder processing methods. Thermosetting polymers are preferred as precursors due to their high molecular weight, ability to prevent uncontrolled polymerization, adequate solubility, functional groups for subsequent reactions, and precise molecular architecture for synthesising stoichiometric ceramic materials like SiC or Si_3N_4. Over the past five decades, various Si-based preceramic polymers with diverse molecular architectures have been developed, with organochlorosilanes being the primary precursors. Examples include polycarbosilanes, polysiloxanes, and polysilazanes, which are produced through reactions with sodium or potassium, water, and ammonia.[110] Making ceramic materials from organosilicon polymer precursors usually involves three main steps: (1) choosing or making an organosilicon polymer with the right composition, structure, and controlled molecular weight, (2) shaping the polymer precursor and then crosslinking it, either through heat or a catalyst, at temperatures between 100 and 300 °C to form an organic/inorganic composite, and (3) heating the crosslinked composite in a controlled atmosphere at temperatures between 500 and 1500 °C to turn it into the final ceramic, which can be either amorphous or crystalline.[111]

Synthesizing preceramic polymers entails the polymerization of monomers that can subsequently be transformed into ceramic materials *via* thermal treatment. A prevalent approach for synthesizing preceramic polymers involves the use of polysiloxanes. This synthesis typically consists of the reaction of silane monomers in conjunction with a catalyst or initiator, resulting in either linear or cross-linked polymers. Additionally, sol–gel techniques may be employed to create preceramic polymers with tailored compositions and structures. The preceramic polymers produced can then undergo thermal treatment, resulting in ceramic materials characterized by high-temperature stability and other advantageous properties. We will now elucidate several of these methods.[112]

4.1 Sol–gel process

The sol–gel method, which involves the hydrolysis and condensation of hybrid silicon alkoxides, can be used to produce crosslinked polysiloxanes, also known as silicon resins, as illustrated in Fig. 3a. This method was first used by early researchers who founded the field of SiOC glasses. The precursors used in this process are organically modified silicon alkoxides, which have the general formula $R_xSi(OR')_{4-x}$. After the gelation phase, these precursors form silicon resins,

$R_xSiO_{(4-x)/2}$. R′ typically represents a CH_3 or C_2H_5 group, while R stands for an alkyl, allyl, or aryl group. By co-hydrolyzing different hybrid silicon alkoxides, the sol–gel method enables precise control over the composition of the original silicon resin.[112] As a result, precursors for silicon-containing organic compounds (SiOCs) that are stoichiometric, excess-C, or excess-Si have been created.

This approach also allows for the uniform incorporation of supplementary elements, such as Al, Ti, or B, into the preceramic network using their respective metal alkoxides.[115] However, the sol–gel process has some limitations, such as poor control over viscosity, which limits the use of shaping methods like extrusion and injection molding. Additionally, the considerable shrinkage during the drying process makes it more challenging to produce samples without cracks. Many researchers are studying the relationship between processing, microstructure, and properties of macroporous SiC materials.[116,117] The main challenges that limit the widespread use of polymer-derived porous SiC materials are the high cost of preceramic polymers, the use of hazardous materials, and the lengthy time required for the synthesis process.[118,119] Sol–gel methods that use affordable carbon-based monomers and silicon alkoxides, followed by pyrolysis, have been widely studied as alternative approaches. However, shrinkage and cracking during the sol–gel process make it difficult to produce bulk SiC materials. To prevent the collapse of bulk gels, expensive drying methods such as supercritical fluid drying and freeze drying, along with long solvent exchange processes, are often used.[113,120,121]

Li *et al.* created organic–inorganic gels that can be turned into SiC hierarchical porous materials by heating them. They employed a simple and cost-effective method involving sodium dodecyl sulfate (SDS) to facilitate sol–gel drying at room temperature (Fig. 3a). The presence of SDS facilitates the coarsening of colloidal particles within the hybrid cell, enabling the formation of three-dimensional solid networks characterized by larger pore sizes. This structural enhancement is advantageous as it mitigates the capillary pressure that typically leads to cracking. The hybrid gels transformed β-SiC upon heating to 1400 °C. The porosity and size of the pores in the macroporous SiC monoliths can be adjusted by changing the amount of SDS used in the hybrid cells. The specific surface area of the SiC monoliths can reach up to 171.5 m^2 $(g)^{-1}$. The compressive strength and Young's modulus of the SiC composites were found to be 7.0 ± 0.8 MPa and 407 MPa, respectively.[113]

4.2 Polymerization methods

Over the past century, methods for producing polymeric organosilicon have undergone significant improvements and expansion. Since silica is found naturally, the monomers for polymeric organosilicon are created through synthetic processes. Silanes have the general formula $R_{4-n}SiX_n$, where X represents reactive groups like Cl, –OR, –OOCR, and $–NR_2$. These groups are essential for starting the polymerization of organosilicon compounds. There are a few ways to make these silanes: (i) by reacting an organic compound directly with silicon at high temperatures; (ii) by chlorinating silicon and then using organic groups and organometallic reagents, such as organolithium compounds, Grignard reagents, and organic zinc compounds; or (iii) by turning silicon into silyl hydrides, which then react with multiple bonds in a hydrosilylation reaction.[122] It's essential to note that hydrosilylation is a key reaction in organosilicon chemistry and has become a primary method for combining organic groups with silicon structures.[123] Polymerization is necessary for the synthesis of preceramic inorganic polymers. Following pyrolysis, these polymers can produce inorganic ceramics, including SiC, Si_3N_4, and SiOC. For example, polycarbosilanes are distinctive precursors for synthesising SiC ceramics and fibres. Traditional manufacturing processes often involve severe reaction conditions and utilize low-molecular-weight compounds, whereas catalytic hydrosilylation polymerization generally relies on noble metal catalysts. Chen *et al.* have documented a cobalt-catalyzed hydrosilylation polymerization process involving dienes and bis-silanes. This approach presents a viable alternative for producing linear polycarbosilanes (Fig. 3b).[57]

4.3 Pyrolysis techniques

Pyrolysis is a thermal degradation process that occurs in the absence of oxygen or an inert environment. This method has been widely employed in various organosilicon polymers, including silicones, polysilanes, and polysiloxanes.[124,125] The resulting materials are utilized in multiple applications, including electronics, coatings, and sealants, owing to their exceptional thermal stability, flexibility, and durability against environmental factors. The PDCs transform a ceramic material *via* a range of thermal techniques. These techniques encompass spark plasma sintering,[126] chemical vapour deposition,[127] rapid thermal annealing,[128] laser pyrolysis,[129] microwave heating,[130] and the predominant method employed, pyrolysis[125] conducted in an Ar or N_2 atmosphere. PDCs represent a highly adaptable category of materials produced through the pyrolysis of silicon-containing polymers. For example, SiOC materials, in particular, are noteworthy due to their distinctive capability to achieve near-net shapes at lower temperatures compared to conventional ceramics. These SiOC systems find diverse applications, including coatings, microwave-absorbing devices, and components designed for high-temperature environments.[131] Among these applications, SiOC-based systems have been the focus of extensive research. The precursor materials typically comprise a Si–O backbone with side groups such as –H, $–CH_3$, $–C_2H_3$, and $–C_6H_5$. At the same time, the pyrolyzed material forms an amorphous SiOC structure with different carbon areas. The transition from polymer to ceramic is a crucial process in which Si–H and Si–C bonds are broken, hydrogen is removed from phenyl rings and $–CH_3$ groups, and new radical species and phases are formed. The various stages that emerge within the system are primarily influenced by the pyrolysis temperature and the choice of precursor(s).

Additionally, during the decomposition of the polymer, several cyclic species can form, including cyclic SiO species,

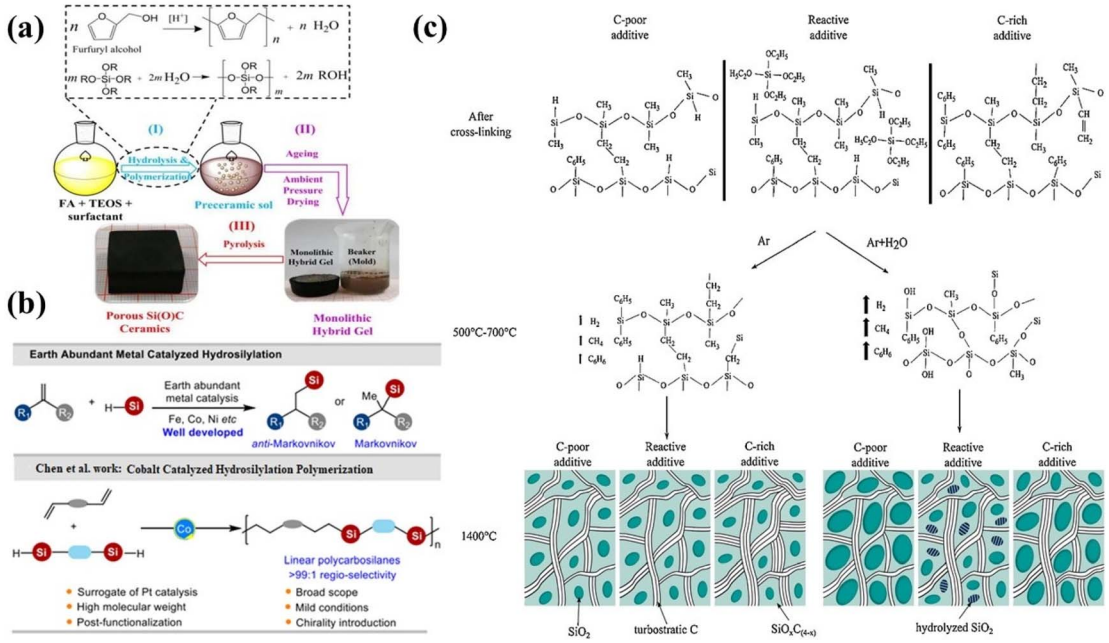

Fig. 3 (a) Schematic representation for synthesising porous SiC-based materials utilizing the sol–gel method. Figure (a) was adapted by permission from: *Materials*, 2022, **16**(1), 220.[113] (b) Earth-abundant metal-catalyzed hydrosilylation. Figure (b) was adapted by permission from: *Macromolecules*, 2024, **57**(16), 8146–8153.[57] (c) Depiction demonstrating the influence of additives and the pyrolysis environment on the microstructure of SiOC. Figure (c) was adapted by permission from: *Journal of the European Ceramic Society*, 2017, **37**(15), 4547–4557.[114]

while some side groups may remain unaffected. Si–Si bond formation may also occur within these cyclic intermediates[125] at approximately 1000 °C; SiOC (or $SiO_{4-x}C_x$, where $0 \leq x \leq 4$) demonstrates an amorphous ceramic network architecture characterized by silicon atoms that are tetra-coordinated in conjunction with carbon and oxygen atoms.[132] Erb *et al.* prepared bulk SiOC materials from a polysiloxane-based system by adding various organic substances and utilizing different pyrolysis atmospheres. They also treated the materials with HF etching (Fig. 3c). The additives changed the material's structure by affecting the formation of SiO_2 nanodomains. SiOC ceramics made in an Ar + H_2O pyrolysis atmosphere had less SiC and more SiO_2 compared to those made in an Ar atmosphere. Adding water vapor during pyrolysis significantly increased the specific surface area. When 10% tetraethyl orthosilicate (TEOS) was added during pyrolysis in an Ar + H_2O atmosphere, the surface area reached 1953.94 $m^2\ g^{-1}$, compared to 880.09 $m^2\ g^{-1}$ for the polysiloxane base treated in Ar. This study examines the principles behind phase composition and development, providing a novel approach to creating materials with exceptionally high surface areas. Using specific pyrolysis atmospheres and organic additives to enhance surface area is a promising method for producing highly porous SiOC ceramics.[114]

5. Potential uses of preceramic inorganic polymers

Different materials can be used for cleaning up the environment, offering various methods to achieve this goal. Given the intricate nature of these materials, their propensity for rapid evaporation, and their restricted reactivity, it is essential to address the containment and breakdown of environmental contaminants. Consequently, contemporary studies have focused on utilizing ceramics to develop innovative strategies for ecological restoration. Inorganic preceramics play a crucial role in various environmental applications, including the detection, monitoring, and quantification of pollutants, as well as their involvement in the prevention, management, and remediation of these contaminants. Numerous ceramic materials are currently under examination for their potential as catalysts in pollution prevention, control, and remediation efforts. Inorganic preceramic materials have emerged as essential components in environmental remediation, attributed to their unique characteristics and versatile applications. This review section examines the body of research concerning ceramics and their diverse ecological applications. Readers are expected to develop a deeper understanding and appreciation of this field through this exploration, which may inform their research endeavours.

5.1 Coatings and composites

It has been reported that preceramic polymers can produce low-dimensional products, particularly coatings.[133] These polymers can be applied to various substrates through various deposition methods, which may utilize liquid or vapour phases. Preceramic polymers can be enhanced by incorporating various fillers to modify specific properties and facilitate the formation of thicker layers without cracking. When fillers are incorporated into a matrix, several technological challenges arise,

particularly when achieving the desired particle fragmentation and uniformity levels. As a result, there are constraints on achieving the requisite layer thickness. This can lead to uncontrolled cracks and pores, which diminish the adhesion between the layer and the underlying surface.[134] It is recommended to make ceramic thin films using unfilled polymer precursors. For instance, the meticulous preparation of the polysiloxane network enables SiOC materials to demonstrate advantageous characteristics, including excellent thermal stability, abrasion resistance, and reduced surface energy.

Furthermore, this process can yield dense layers that protect coatings in challenging environments, such as those exposed to corrosive gases with moisture at elevated temperatures or radiation.[135,136] Research on synthesising polysiloxane films devoid of additive incorporation has encountered difficulties related to the alteration of precursors and the structural stability of the resultant materials. This problem is attributed to the use of unmodified polysiloxanes or small alkoxysilanes with only one Si atom during the sol–gel polymerization process.[137,138] While achieving a well-defined precursor structure is possible, this necessitates the use of monomers that possess multiple Si atoms and substantial quantities of solvent to address the diminished solubility in water.[139]

Malinowska *et al.* created SiOC layers on stainless steel surfaces using polysiloxane networks without the addition of fillers (Fig. 4a–e). This approach minimizes shrinkage during the pyrolysis process. It improves the adhesion of the SiOC layer to the substrate—the design of the precursor aimed to reduce weight loss during annealing, thereby achieving material shrinkage. The cross-linking of polymers to create precursor coatings was accomplished through a hydrosilylation reaction. Given that this reaction necessitates the presence of asymmetric groups, two distinct SiOC coatings were developed on stainless steel, resulting from the thermal decomposition of the polymer precursors polymethylvinylsiloxane/2,4,6,8-tetramethylcyclotetrasiloxane (V_3/D_4^H) and polymethylhydrosiloxane/1,3,5,7-tetravinyl-1,3,5,7-tetramethylcyclotetrasiloxane ($PMHS/D_4^{Vi}$). Applying SiOC layers on the chosen steel substrate significantly improved its harsh temperature corrosion resistance, with the one coated with $pyroV_3/D_4^H$ exhibiting superior oxidation resistance compared to the one coated with $PMHS/D_4^{Vi}$. Without a protective coating, a clear difference in corrosion resistance is observed between layers made from precursors with vinyl groups in the polymer chain ($pyroV_3/D_4^H$) and those linked to the cross-linking agent ($PMHS/D_4^{Vi}$). This difference is primarily due to the latter having more microcracks. These microcracks happen because the Si–H bonds in PMHS are blocked, which slows down the material buildup during the spin coating process. Additionally, lower bonding density makes the material more likely to form microcracks.[134]

Fig. 4f and g illustrates notable variations in layer morphology contingent upon the precursor utilized. In contrast to the $PMHS/D_4^{Vi}$ layer, the V_3/D_4^H layer exhibits sporadic cracking, characterized by a uniform coating with minimal defects. The occurrence of cracks in the thicker layer (~1.7 μm) of V_3/D_4^H (Fig. 4h) can be attributed to the coating's thickness, which also influences the thermal evolution of the layer. During the pyrolysis process, the polymer precursor undergoes a mass transformation and experiences an increase in density. This transformation leads to in-layer shrinkage, which subsequently results in the formation of cracks. Bulky layers are particularly susceptible to this phenomenon, thereby imposing a limitation on the achievable layer thickness.

Conversely, the layer formed from the PMHS polymer is significantly thinner, with a maximum thickness of approximately ~450 nm (as shown in Fig. 4i), indicating a reduced impact of shrinkage on thinner layers. It is essential to highlight that, despite the presence of cracks, the layer maintains a uniform structure and exhibits strong adhesion to the metal substrate.[134] Furthermore, the process temperature can be kept at relatively low levels (below 800 °C) to minimize the risk of harm to the underlying substrate. Finding low-temperature and financially feasible methods to shield metal surfaces from oxidation, wear, and corrosion is a top priority. Although the interactions at the interface during processing might enhance adherence to the metal, it is crucial to prevent the formation of brittle phases—coatings created by incorporating silicon or carbon clusters, which may be suitable for optoelectronic applications. Carbon fibres and carbon/carbon composites are coated with oxidation protective layers.[140] By incorporating fillers, layers with controlled porosity can be fabricated, making them suitable for use as catalyst supports or in biomedical systems. The application of preceramic layers processed at low temperatures is particularly noteworthy for their ability to coat extensive surfaces, such as train carriages. These layers form transparent, strong coatings that stop inks, permanent markers, spray paints, stickers, dirt, and other contaminants from sticking.

They also help protect against weathering, corrosion, and oxidation. In addition, preceramic polymer films have been successfully used as a bonding agent for ceramic matrix composites and solid ceramic materials.[141] In this context, the incorporation of fillers plays a crucial role in reaching desirable characteristics and an appropriate microstructure within the ceramic interlayer. Barroso *et al.* created a dual-layered thermal barrier coating (TBC) system utilizing polysilazane, comprising both a bond coat and a top coat. The upper layer combines passive fillers like YSZ and active ones like $ZrSi_2$ within an (organic)silazane matrix. The top coat application onto steel substrates was achieved through tape casting, a method noted for its excellent reproducibility and minimal use of suspension. Following the removal of solvents at 110 °C, the coatings and their constituents underwent pyrolysis for one hour at temperatures of 500 °C and 1000 °C, respectively, for the top coats. After this, they were subjected to further investigation. The findings indicated that when subjected to temperatures exceeding 500 °C, $ZrSi_2$ undergoes a controlled oxidation process, resulting in the formation of thermally stable ZrO_2 and SiO_2 phases. These phases serve as protective barriers, preventing further degradation in oxidative environments up to 1000 °C. Moreover, the volumetric expansion resulting from the oxidation of $ZrSi_2$ effectively offsets the natural shrinkage of

polymers during pyrolysis, leading to the development of dense and crack-free coatings.

In contrast, coatings that consist solely of passive fillers, such as YSZ, demonstrate significant cracking and compromised structural integrity due to the absence of reactive compensation mechanisms. The synergistic integration of both active and passive fillers enhances thermal expansion compatibility with metal substrates and mitigates thermal mismatch stresses. These results underscore the essential function of active fillers such as $ZrSi_2$ in optimizing the thermo-structural performance of PDC-based TBC systems for prolonged high-temperature applications.[142]

Niu *et al.* created a $MoSi_2$–SiOC–Si_3N_4 (MSS) coating on SiC-coated C/C composites using a slurry method. The slurry was made by mixing $MoSi_2$ and Si_3N_4 powders in high hydrogen silicone oil (H–PSO), with tetramethyl tetravinylcyclotetrasiloxane (Vi-D_4) as the cross-linking agent and platinum chloride as the catalyst. The coating was heat-treated at 1000 °C for 2 hours in nitrogen gas to form MSS, with an average thickness of 140 μm. They also made a $MoSi_2$–SiOC outer coating using the same slurry method for comparison. The oxidation behavior of the C/C composites with different outer coatings was tested at 1500 °C in air. The results showed that the MSS coating provided better protection against oxidation than the $MoSi_2$–SiOC coating. Additionally, the antioxidant properties of the MSS coatings are strongly influenced by the amount of Si_3N_4.[143]

5.2 Removal of environmental pollutants

A lot of research is currently focused on creating new adsorbents and improving their ability to adsorb. Preceramic polymers offer numerous benefits because their molecular structure can be easily modified, and they can be shaped into various forms using plastic-forming methods.[144] Materials made from preceramic polymers can be modified to function as effective adsorbents for removing heavy metals such as lead (Pb), mercury (Hg), and arsenic (As) from industrial wastewater.[145] These materials' high surface area and chemical versatility make them suitable for capturing toxic ions. Polysiloxanes are recognized as the most cost-effective among all polymeric precursors. Their availability is high and can be processed under normal atmospheric conditions. Amorphous SiOC can be made by heating it to temperatures between 800 and 1400 °C. It remains an undeniable fact that there is a notable lack of scientific literature on the specific applications of porous and high-surface-area PDCs. Recently, materials derived from complex processing methods, including PDCs aerogels[146] and composites created from polysiloxane and wood,[147] have been evaluated for their efficacy as dye adsorbents.[148] Zeydanli *et al.* produced a SiOC with exceptional permeability and a large surface area achieved through a preceramic polymer blend combined with a catalyst. Following the annealing and thermal decomposition processes, specific samples underwent etching with HF to yield carbon-rich SiOC (C-rich SiOC), which was explicitly identified as sample W–HF.

W and W–HF were first tested to assess their ability to remove heavy metals, particularly Cr(III), Pb(II), and Cd(II), as well as

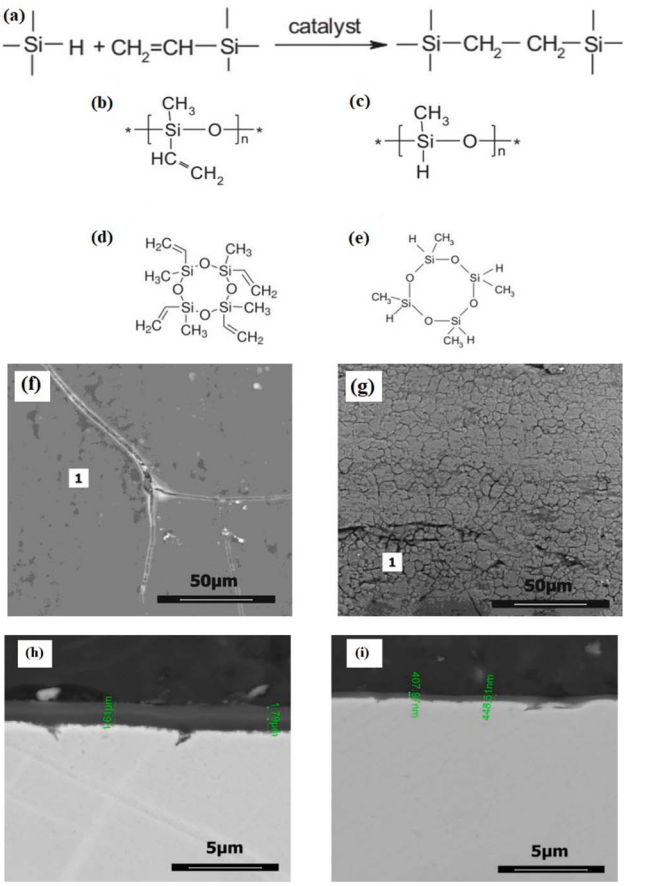

Fig. 4 (a) Schematic illustration of the hydrosilylation process, along with the structural representations of the compounds utilized in the research, (b) V_3 polymer, (c) PMHS polymer, (d) D_4^{Vi}, (e) D_4^{H}. SEM images depicting the surface morphology of steel coated with SiOC layers: (f) pyroV_3/D_4^{H}, (g) pyroPMHS/D_4^{Vi}. Also, cross-section SEM images of steel coated with SiOC layers: (h) pyroV_3/D_4^{H}, (i) pyroPMHS/D_4^{Vi}. Figures (a)–(i) were adapted by permission from: *Surface and Coatings Technology*, 2021, **407**, 126760.[134]

cationic dyes such as methylene blue (MB), rhodamine B (RhB), and crystal violet (CV). The tests were done separately and in combinations. HF-treated SiOC samples with high surface area showed a strong ability to adsorb cationic dyes. The higher adsorption of dyes, compared to metal ions, is due to the Si–OH bonds, which are more common in HF-treated SiOC and free carbon. These bonds interact with organic dyes through (a) van der Waals forces between the dyes and the sp^2 hybridized carbon, and (b) electrostatic interactions involving Si–OH groups and carbon–oxygen complexes.[149] Research conducted over the last thirty years identified Si_3N_4 as one of the most durable and resilient ceramic materials for structural applications. However, recent investigations have revealed its extraordinary surface biochemistry in the present century. This paper provides a comprehensive overview of the potential applications of Si_3N_4 in various fields, including disease diagnosis and treatment, personalized healthcare, agricultural practices, food and water safety, and environmental conservation.[150] Si_3N_4 exhibits a notable ability to support metal oxides, thereby preventing

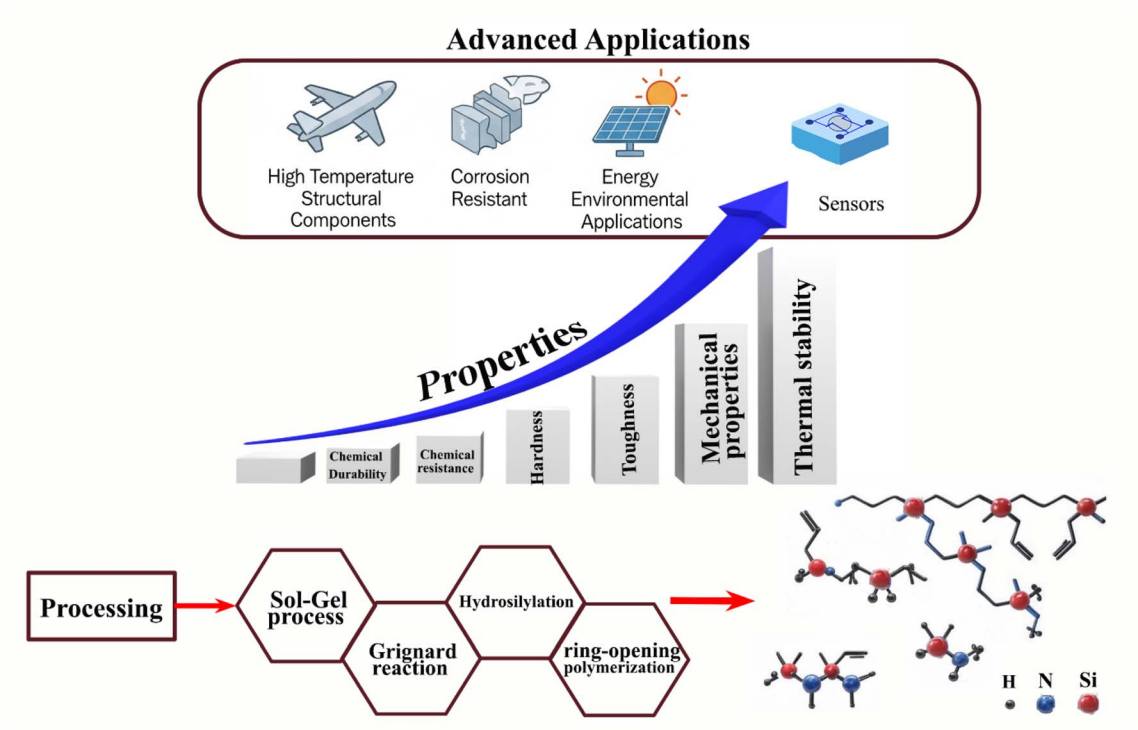

Fig. 5 Schematic diagrams summarizing synthesis methods and advanced applications.

agglomeration of these oxides. Si_3N_4 exhibits many remarkable characteristics, including exceptional oxidation resistance, significant mechanical strength, impressive thermal stability, and low density. In the realm of photocatalytic activities, it serves a vital role as a support material that facilitates the reduction of charge recombination and enhances the efficient transport of charge carriers. Based on this, Sharma *et al.* have developed a Fe_3O_4/ZnO/Si_3N_4 nanocomposite, which may serve as an effective photocatalyst. The photocatalytic performance of the material has been investigated for the degradation of yellow sunset and methyl orange (MO) in aqueous solutions. The findings indicated that the degradation efficiencies exceeded 90% for sunset yellow and 96% for MO. Inhibition experiments revealed that hydroxyl radicals (˙OH) play a crucial role in the degradation mechanism. Furthermore, a reusability assessment conducted over six consecutive cycles demonstrated sustained photocatalytic activity, highlighting its effectiveness even after multiple uses. Additionally, antimicrobial tests performed on *E. coli* and *Pseudomonas* strains exhibited a notable inhibition zone.[151]

Polysilsesquioxane (PSQ) represents a class of organic–inorganic hybrid materials characterized by a backbone of Si–O inorganic bonds complemented by organic groups in the side chains. This unique composition and structural arrangement endow PSQ with remarkable properties. Notably, the organic groups attached to silicon can participate in various chemical reactions, enabling further functionalization. Moreover, PSQ exhibits exceptional resistance to corrosion, impressive thermal stability, and notable chemical reactivity, making it suitable for applications in semiconductor technology, catalysis, adsorption, and other domains. As an adsorbent, PSQ typically demonstrates a high capacity and rapid rate of adsorption.[145] Research conducted by Niu *et al.* involved the synthesis of a thiol-functionalized PSQ designed explicitly for the adsorption of Hg(II) and Mn(II) ions from solutions.[152] Additionally, Wang *et al.* synthesized two unique varieties of fibrous adsorbents through the application of thiol- and amino-functionalized PSQ onto poly(*p*-phenyleneterephthalamide) fibres and subsequently evaluated their effectiveness in the adsorption of Hg(II).[153]

Xu *et al.* created magnetic composites of PSQ/CNTs using the sol–gel method, which involved carboxylic carbon nanotubes (CNTs–COOH), 3-aminopropyl-trimethoxysilane (APTMS), and 3-mercaptopropyl-trimethoxysilane (MPTMS). At the same time, they added magnetite to the composites to improve their ability to separate from water. These composites were used to recover Au(III) from wastewater, and the results showed that the PSQ/CNTs magnetic composites were very effective at adsorbing Au(III).[145]

5.3 Microwave absorption

The rapid growth of electronic devices and information technology has led to extensive research on materials that can mitigate the harmful effects of interference and radiation caused by electromagnetic waves (EMW).[14] In particular, ceramics produced through the PDC method have garnered significant attention in recent research due to their improved capabilities in microwave absorption and electromagnetic field (EMF) shielding. Recent years have witnessed rapid progress in

Table 2 Potential uses of preceramic inorganic polymers (preparation method, morphology, application, and advantages)

Preparation method	Nanocomposite	Morphology	Application	Advantages	Ref.
Pyrolysis	Ni/SiOC(H) nanocomposites	A homogeneous blending of the composites	Removal of acid fuchsin	The OCMC–CS films showed improved adsorption characteristics compared to OCMC–CS–SiC and OCMC–CS–SiC@SiO_2 films. At the same time, incorporating SiC and SiC@SiO_2 nanoparticles conferred certain structural advantages that reduced the overall adsorption capacity	171
Oxidation and casting method	OCMC–CS–SiC@SiO_2 nanocomposite film	A porous and interconnected network that becomes less porous upon the incorporation of SiC@SiO_2 nanoparticles	MB dye adsorption	• The film presents a hopeful and eco-friendly answer for reducing dye contamination in water-based systems • The presence of SiC or SiC@SiO_2 in OCMC–CS led to a reduction in adsorption efficiency, which was unexpected • The decline in adsorption effectiveness may be attributed to the interplay between polymer functional groups and SiC or SiC@SiO_2 nanoparticles, reducing accessibility for MB dye adsorption • The decline in adsorption effectiveness is corroborated by the observation that including SiC or SiC@SiO_2 in pristine CS polymer enhanced adsorption efficiency, suggesting augmentation of surface functionalities and surface area within CS films	172
Electrospinning followed by heat treatment	SiC-doped Yb_2O_3 structure	Nanofibers	Photocatalytic hydrogen evolution reactions	• The increased activity level can be credited to the biopolymer's combined impact (cellulose or chitosan) and the inorganic catalyst (Yb_2O_3/SiC) • Cellulose and chitosan function as mediators and bio-templates in the photocatalytic water splitting reaction, which augments the photocatalytic activities of bio-templated catalysts	173
Vat-based photopolymerization	Polymer-derived Ni/SiOC materials	Film	CO_2 methanation	• A new method for making Ni-modified polymer-derived SiOC using vat-based photopolymerization in 3D printing is introduced • The SiOC/Ni composites display catalytic properties that are appropriate for the methanation of CO_2 • The SiOC/Ni materials that can be printed offer a promising approach to combining metal-modified polymer-derived ceramics with 3D printing, particularly for applications in catalysis	174

Table 2 (*Contd.*)

Preparation method	Nanocomposite	Morphology	Application	Advantages	Ref.
Slow dip coating approach	SiOC ceramic composite membranes	Layered structure	Water purification	• The SiOC composite nanofiltration membranes showed strong mechanical strength and remained stable for long periods during cross-flow filtration • The gradual immersion coating method enhanced the spreading and even distribution of the solution on the surface, resulting in a thick SiOC separation layer • The SiOC-1 composite nanofiltration membrane demonstrated a permeate flow rate of 8.97 L m^{-2} h^{-1} bar^{-1} and a significant dye molecule rejection rate of 95.1% • The potential applications of SiOC ceramic membranes with reduced sintering temperature are numerous and promising for future development	175
Co-electrodeposition process	Si_3N_4–PbO_2 nanocomposite	Multilayer heterojunction – the pyramidal shape of a typical β-PbO_2 structure, which steadily decreases as the concentration of Si_3N_4-doping nanoparticles increases, enhances the crystallinity of lead dioxide	Electrocatalytic degradation of sulfathiazole	• The Si_3N_4–PbO_2 electrode was used as the anode in breaking down sulfathiazole-simulated and natural sulfonamide wastewater through electrocatalysis • The introduction of 6 g L^{-1} of Si_3N_4 resulted in a notable enhancement in the durability of the lead dioxide electrode, enabling it to operate for 94 hours • The electrocatalytic degradation process using the novel electrode is considered environmentally friendly for water treatment	176
Vacuum hot-pressing at 1800 °C	SiCw/Si_3N_4 composite	The SiC whiskers are uniformly distributed at the Si_3N_4 grain boundaries and have a long, rod-shaped morphology	Microwave absorption	• SiCw incorporation led to grain refinement, elevated grain aspect ratio (GAR), and diminished average grain size (GAvg) in Si_3N_4 • Adding SiCw significantly improved the mechanical properties of the ceramic material • Better microwave absorption was achieved because of the dielectric loss from the SiC phase and good impedance matching • Adding SiCw to the Si_3N_4 matrix results in improved mechanical properties of the ceramics and an enhanced ability to absorb microwave wavelengths	177

Table 2 (*Contd.*)

Preparation method	Nanocomposite	Morphology	Application	Advantages	Ref.
Solvent-thermal method and *in situ* polymerization	MWCNT/Si_3N_4/PANI ternary composites	Carbon nanotubes (CNTs) are adhered to and intertwined on the exterior of Si_3N_4 and PANI clusters	Microwave absorption	• The presence of a conductive network involving MWCNT, Si_3N_4, and PANI contributes to an increase in conductive loss • The composites display several loss mechanisms and excellent impedance matching • The feeding ratio 3 : 20 : 40 for MWCNT : Si_3N_4 : PANI resulted in an optimal reflection loss (RL) of −42.57 dB at 8.8 GHz • By incorporating Si_3N_4, the composites can display satisfactory resistance to elevated temperatures	178
One-pot method of single-source precursors	Amorphous SiBCN	Hierarchical structure	Microwave absorption	• By adjustment of carbon content, the microwave absorption properties of amorphous SiBCN ceramics were enhanced • Up to 1400 °C, the amorphous ceramic materials showed excellent stability • Its hierarchical structure and nano boundaries improve its electromagnetic wave attenuation capabilities • The maximum adequate absorption bandwidth was 4.07 GHz at a thickness of 2.80 mm	167
Polymer infiltration pyrolysis method	Ti_3SiC_2 modified SiC_f/BN/SiBCN composites		The EMI shielding	• The material exhibited a notable combination of impedance matching and electromagnetic loss at 1400 °C oxidation, leading to the optimal electromagnetic interference shielding effectiveness	179
Controlled impregnation–pyrolysis cycle method	SiCN(Fe)/Al_2O_3 composite ceramics	The porous matrix	Electromagnetic wave absorption	• Enhancing iron and carbon can improve magnetic and dielectric losses, thereby enhancing the material's absorption properties • The sample absorbs approximately 99% of the electromagnetic waves with 3 wt% FeAA at 1000 °C, with a reflectivity of −18 dB at 12 GHz	180
Electrospinning and pyrolysis	SiCN/C fibers	Fibres	Microwave absorption and EMF shielding in Ku-band	• SiCN/C fibres are lightweight ceramic materials that are resistant to corrosion and heat • The fibres offer superior EMF protection within the Ku-band frequency range of 12.4–18 GHz	164

Table 2 (*Contd.*)

Preparation method	Nanocomposite	Morphology	Application	Advantages	Ref.
Ball mill and pyrolysis	SiBCN ceramics	A rough, porous, and randomly distributed microstructure	Temperature sensor	• SiBCN ceramics have a sensitivity of 3.5% per K from room temperature to 980 °C, with B-values reaching up to 3118 K • The SiBCN sensor exhibits a more rapid rate of temperature response • The SiBCN ceramic temperature sensor is ideal for accurately measuring temperatures in extremely high heat and harsh environments	181
Solvothermal, freeze-casting and pyrolysis	rGO reinforced SiBCN aerogels	SiBCN macroblocks form a necklace-like 3D structure interwoven with rGO nanosheets	Thermal insulation	The rGO/SiBCN aerogels provide excellent thermal insulation, withstand high temperatures, resist ablation, and remain stable in different conditions. They can resist oxidation at 800 °C in still air and maintain their structure at 1200 °C in an argon gas environment	182
RF magnetron sputtering	Cu/SiC/Si photo-sensor	Thin film	High-temperature devices	• The nanocrystalline thin film demonstrates a high level of efficiency in absorbing light • The occurrence of traps that lead to extra photocurrents • The photodetector's exceptional responsivity is a result of the combination of various elements	183

the development of microwave absorption materials, which significantly diminish the strength of incoming electromagnetic waves. This plays a crucial role in implementing stealth technology within the defense and security sectors. Among these, ceramic materials, characterized primarily by their dielectric loss, exhibit distinctive physicochemical properties. The distinctive oxidation resistance and remarkable stability at elevated temperatures of ceramics make them more advantageous than alternative materials for application as microwave absorption substances, especially in modern high-temperature and demanding conditions.[154] PDCs represent a method for producing microwave-absorbing ceramics *via* a conversion process that transforms polymers into ceramics. The unique characteristics of polymers and ceramic materials enable the use of PDCs in fabricating a wide range of microwave-absorbing ceramics. This is achieved through various processing techniques, including fibres, composites, powders, and specialized structures created through 3D printing. SiCN ceramics have attracted considerable attention in Si-based PDCs in recent decades, mainly owing to their enhanced thermal and oxidation resistance relative to SiOC and SiC ceramics.

Recent developments in the utilization of ceramics derived from polysilazane for electromagnetic interference (EMI) absorption have led to the creation of various composites, including SiCN,[155] SiCN/Fe,[156] and SiCN/Ni.[157] The electrospinning technique, combined with subsequent thermal processing, has been utilized for the template-free production of PDC fibers exhibiting EMF absorption characteristics.[158] Incorporating ferric and nickel compounds into SiCN fibers typically induces magnetic loss,[159,160] which may lead to increased weight density, susceptibility to corrosion, processing challenges, and elevated costs. Incorporating carbon into SiCN ceramics can enhance dielectric characteristics, facilitate the production of lighter materials, and bolster resistance in harsher environments. The effectiveness of EMF shielding provided by PDC fibres integrated with carbon has been demonstrated in various studies, including those SiC/Si_3N_4 fibres that incorporate *in situ* embedded graphite,[161] C/SiC fibres,[162] graphite–SiC wires.[163] Ramlow *et al.* investigated the microwave absorption and EMF shielding characteristics of electrospun SiCN/C fibres. A hybrid approach utilizing electrospinning alongside the PDC method was implemented to produce SiCN fibres, which integrated carbon structures formed *in situ*. This fabrication technique was specifically designed for applications related to microwave absorption and EMF shielding within the Ku band (12.4–18 GHz). For comparative purposes, additional SiCN fibres were synthesized. In this process, polysilazane was used to provide SiCN. At the same time, PAN was added to the solution to improve the electrospinning of the ceramic-filled polymer and serve as a carbon source. The analysis of the samples revealed varying trends in EMF shielding effectiveness, specifically regarding their reflection, transmission, and absorption characteristics. Notably, incorporating carbon into the SiCN matrix resulted in a doubling of EMF absorption compared to SiCN fibres alone. The SiCN/C fibres exhibited a minimum reflection coefficient (S_{11}) of −12 dB, indicating a high shielding efficiency that effectively blocked over 90% of EMF energy.

In contrast, SiCN fibres exhibited an S_{11} value of −7 dB, translating to roughly 80% attenuation of EMF energy. Computational simulations further elucidated the superior electromagnetic shielding properties of SiCN/C relative to SiCN, attributing this enhancement to increased conduction losses from the presence of free conductive carbon and diminished dipole and surface polarization effects due to defects. The fibres demonstrated resilience against acidic and alkaline conditions, as well as oxidation, at temperatures of up to 600 °C. Additionally, incorporating a carbon source resulted in a 17% reduction in weight for SiCN/C fibres compared to SiCN fibres. This study presents a viable method for producing SiCN/C fibres with EMF absorption characteristics, suitable for application as lightweight materials in challenging environments.[164]

Another Si-based PDC, quaternary PDC SiBCN, noted for its exceptional high-temperature stability and resistance to oxidation, stands out as the primary material in the realm of high-temperature microwave absorption ceramics documented in the literature. Currently, to address the issue of low dielectric loss associated with PDC–SiBCN, many researchers are enhancing EMW attenuation through the incorporation of high dielectric-loss materials such as carbon-based materials or by employing transition metals like iron and hafnium to catalyze *in situ* crystallization processes.[165,166] For composite materials, filler distribution has consistently been a challenge. Even though transition metals help transform amorphous SiBCN ceramics into crystals, oxidation resulting from phase separation weakens the ceramic's resistance to oxidation. Creating amorphous SiBCN ceramics with microwave-absorbing properties *via* a single-source precursor exemplifies a novel strategy to overcome the constraints associated with the techniques above. Luo *et al.* conducted a study in which they developed amorphous SiBCN ceramics for microwave absorption applications. This was achieved using a single-source hyperbranched polyborosilazane containing benzene rings, utilizing a one-pot synthesis approach. Dichlorodiphenylsilane increased carbon incorporation in the pyrolyzed SiBCN ceramics and improved the ordered carbon ratio. Changing the monomer ratio and heating temperature of the ceramic material produced PDCs with strong microwave absorption properties while maintaining their structure. This process resulted in a lowest reflection coefficient (RC_{min}) of −30.79 dB and a good absorption bandwidth (EAB_{max}) of 4.07 GHz.

Furthermore, the PDC-derived SiBCN ceramics exhibited remarkable thermal stability, showing negligible mass loss in Ar and air atmospheres up to 1400 °C. This innovative and efficient method for preparing PDC–SiBCN materials holds promise for large-scale production. It offers new perspectives for developing microwave absorption materials suitable for extreme conditions.[167]

5.4 Sensors for environmental monitoring

Sensors play a crucial role in advanced systems that necessitate detection and regulation. The research conducted by Nagaiah *et al.* investigates the applicability of high-temperature heat flux (HTHF) sensors within gas turbine systems. They have effectively engineered and fabricated these sensors by leveraging

recent innovations in a novel ceramic material sourced from PDCs. The PDC–HTHF sensor was developed using SiCN, which was synthesized from an innovative polymer *via* lithography. This method was proposed as a viable microfabrication technique for sensor production, with conductivity regulated through the careful selection of composition and treatment parameters. SiCN sensors preserve their structural and functional integrity in extremely high-temperature conditions due to a combination of inherent material stability, electrical tunability, and versatile fabrication methods. The amorphous SiCN matrix demonstrates remarkable thermal and oxidation resistance, maintaining stability at temperatures surpassing 1400–1500 °C, even in reactive environments such as combustion gases or turbine flows.

Additionally, these ceramics provide adjustable electrical conductivity and a high temperature coefficient of resistance (TCR), with values reaching up to 4000 ppm per °C, facilitating dependable thermal sensing throughout extensive thermal cycling. Structurally, the monolithic, crack-free design achieved *via* direct pyrolysis of preceramic polymers eliminates interfacial failures that are typical in multilayered or bonded systems. Moreover, compatibility with lithographic and microlithographic fabrication techniques enables the precise integration of SiCN sensors onto complex microscale surfaces.

In contrast, traditional heat flux sensors that utilize metal films or wires are constrained by lower thermal thresholds (approximately 1100 °C), susceptibility to oxidation, and mechanical fragility. Consequently, SiCN-based PDC sensors offer a robust and scalable alternative for high-temperature sensing applications in aerospace, energy, and thermal protection systems.[168] Additionally, PDC sensors are produced due to their semiconducting properties, particularly their temperature-dependent conductivity. SiC sensors have found extensive application in environments with temperatures not exceeding 500 °C. PDC sensors can function as reliable high-temperature microsensors, utilizing the PDCs' piezoresistive principle or doping, which requires sensing materials to withstand harsh environments at high temperatures without compromising their functionality and structure.[169] Developing strain sensors that exhibit high responsiveness across a broad spectrum of temperatures and strains remains a significant challenge, particularly in high-temperature conditions. Yang *et al.* have introduced a dual-functional sensor featuring a beam concealer structure constructed from polymer-derived SiCN ceramics capable of monitoring temperature and strain. The performance of this integrated sensor was evaluated across a temperature range extending from ambient conditions to 1000 °C, with a comprehensive investigation of the fundamental sensing mechanism. The resulting strain sensor demonstrated an impressive response time of 60 ms within a strain range of 0–3500 με, with a maximum strain rate reaching 46 200 με S^{-1}.

Furthermore, this sensor exhibited remarkable stability and exceptional sensitivity in high-temperature environments. Notably, temperatures can be detected independently up to 1000 °C without interference. With its competitive sensitivity, outstanding stability, rapid response time, and extensive operational range, this innovative integrated sensor is promising for detecting temperature and strain signals in practical applications within extremely high-temperature settings.[170] Fig. 5 illustrates the schematic diagrams summarizing synthesis methods and advanced applications. Table 2 represents the potential uses of preceramic inorganic polymers (preparation method, morphology, application, and advantages).

6. Conclusion and future prospects

PDCs constitute a fascinating category of advanced materials, characterized by their distinctive blend of structural integrity, adjustable functionality, and high-temperature resilience. In the last fifty years, these materials have garnered increasing interest due to their potential applications in extreme environmental and industrial settings. This review has explored the current status and emerging capabilities of PDCs in environmental contexts, focusing on their microstructural properties, the processes of ceramic transformation, and the interactions between dopants and fillers. There has been an increasing focus on combining PDCs with innovative methods, including 3D printing, utilizing ceramics derived from biomass, and investigating the biocompatibility of functionalized PDCs.

Despite notable advancements, various limitations continue to obstruct the comprehensive implementation of PDCs. Specifically, a significant portion of existing research remains limited to controlled laboratory environments, lacking adequate long-term performance data in complex, real-world conditions. Obstacles remain in attaining enduring mechanical durability, resistance to oxidation, and functional reliability under cyclic thermal stresses and chemically hostile atmospheres. Likewise, although PDCs have demonstrated potential in MEMS and high-temperature sensor applications, additional miniaturization and system integration are still restricted by present fabrication capabilities and cost-related issues.

To address these challenges, forthcoming studies should adopt a multi-disciplinary strategy. The creation of doped or multi-phase PDC systems featuring delayed crystallization and improved oxidation resistance will be crucial for enhancing durability. Additionally, the progress in scalable, cost-effective preceramic polymer synthesis and solvent-free processing techniques is essential for facilitating high-volume production. Methods such as additive manufacturing, micro-stereolithography, and ink-based printing provide promising avenues for producing intricate sensor designs with reduced waste and enhanced performance. Simultaneously, the integration of PDCs with innovative technologies—including the utilization of bio-derived precursors and the investigation of biocompatibility in functionalized PDCs—offers exciting new possibilities for expanding their range of applications.

As research on PDC progresses, global initiatives are increasingly directed towards customizing these materials for multifunctional applications in extreme conditions. The integration of material innovation, precise fabrication, and functional synergy is set to pave the way for the next generation of high-performance PDCs, solidifying their role as essential facilitators of future technologies in aerospace, energy, electronics, and environmental monitoring.

Abbreviations

PCIPs	Preceramic inorganic polymers
PDCs	Polymer-derived ceramics
SiC	Silicon carbide
Si_3N_4	Silicon nitride
BN	Boron nitride
Al_2O_3	Aluminum oxide
ZrO_2	Zirconium oxide
AIN	Aluminum nitride
SiO_2	Silicon oxide
SiOC	Silicon oxycarbide
SiCN	Silicon carbonitride
AM	Additive manufacturing
Mg	Magnesium
PDMS	Polydimethylsilane
PDMMPS	Polydimethyl-methylphenylsilane
PDMMS	Polydimethyl-methylsilane
κ	Thermal conductivity
CTE	Coefficient of thermal expansion
C_p	Specific heat capacity
α	Thermal diffusion rate
TSR	Thermal shock resistance
BNNTs	Boron nitride nanotubes
PUMVS	Poly(ureamethylvinyl)-silazane
TBC	Thermal barrier coating
PHPS	Perhydropolysilazane
DCP	Dicumyl peroxide
PBDPS	Poly-borodiphenylsiloxane
DPDCS	Diphenyldichlorosilane
PAlC	Polyaluminocarbosilane
PSQ	Polysilsesquioxane
OSR	Organosilane slurry residue
PEO	Polyethylene oxide
K_{IC}	Fracture toughness
PAN	Polyacrylonitrile
SDS	Sodium dodecyl sulfate
V_3	polymethylvinylsiloxane
D_4^H	2,4,6,8-Tetramethylcyclotetrasiloxane
PMHS	Polymethylhydrosiloxane
D_4^{Vi}	1,3,5,7-Tetravinyl-1,3,5,7-tetramethylcyclotetrasiloxane
EMW	Electromagnetic wave
EMF	Electromagnetic field
C	Carbon
O	Oxygen
N	Nitrogen
B	Boron
H	Hydrogen
Al	Aluminium
CH_2	Methylene group
[N=C=N]	Carbodiimide group
NCs	Nanocomposite
N_C	Nitrogen dopant
LB	Lamp black
GR	Graphite
CB	Carbon black
AC	Activated carbon
C_{def}	Defect concentration
PU	Polyurethane
PEO	Polyethene oxide
SiOCs	Silicon carbon oxides
HF	Hydrofluoric acid
SiOCs	Silicon-containing organic compounds
SDS	Sodium dodecyl sulfate
TEOS	Tetraethyl orthosilicate
PMHS/D_4^{Vi}	Polymethylhydrosiloxane/1,3,5,7-tetravinyl-1,3,5,7-tetramethylcyclotetrasiloxane
TBC	Thermal barrier coating
MSS	$MoSi_2$–SiOC–Si_3N_4
H–PSO	Hydrogen silicone oil
Pb	Lead
Hg	Mercury
AS	Arsenic
C-rich SiOC	C-rich SiOC
MB	Methylene blue
RhB	Rhodamine B
CV	Crystal violet
MO	Methyl orange
$^{\bullet}OH$	Hydroxyl radicals
CNTs–COOH	Carboxylic carbon nanotubes
APTMS	3-Aminopropyl-trimethoxysilane
MPTMS	3-Mercaptopropyl-trimethoxysilane
EMI	Electromagnetic interference
RC_{min}	Reflection coefficient
CNTs	Carbon nanotubes
G_{AR}	Grain aspect ratio
G_{Avg}	Average grain size
R_L	Reflection loss

Data availability

The data supporting the findings of this review can be obtained from the corresponding author upon request. Due to privacy concerns and other restrictions, the data are not publicly accessible.

Author contributions

M. M. S. ideation, search, resources, and writing. M. M. conceptualization, supervision, graphics, and editing. A. R. A. review and editing. M. B. review and editing. A. M. co-supervision, project administration, and editing. E. N. Z. co-supervision, project administration, and editing.

Conflicts of interest

The authors declare no conflict of interest.

Acknowledgements

The authors are thankful for the partial support of the Iran University of Science & Technology (IUST).

References

1 C. Vakifahmetoglu, D. Zeydanli and P. Colombo, *Mater. Sci. Eng., R*, 2016, **106**, 1–30.
2 T. Lacelle, K. L. Sampson, H. Yazdani Sarvestani, A. Rahimizadeh, J. Barroeta Robles, M. Mirkhalaf, M. Rafiee, M. B. Jakubinek, C. Paquet and B. Ashrafi, *APL Mater.*, 2023, **11**(7), 070602.
3 Q. Wen, Z. Yu and R. Riedel, *Prog. Mater. Sci.*, 2020, **109**, 100623.
4 K. Zhong, Z. Wang, J. Cui, X. Yu, Z. Yu, Y. Wang, Z. He, Y. Zhao and J. Zhao, *Ceram. Int.*, 2024, **50**, 36521–36536.
5 A. Dorieh, M. F. Pour, S. G. Movahed, A. Pizzi, P. P. Selakjani, M. V. Kiamahalleh, H. Hatefnia, M. H. Shahavi and R. Aghaei, *Prog. Org. Coat.*, 2022, **165**, 106768.
6 Y. Arai, R. Inoue, K. Goto and Y. Kogo, *Ceram. Int.*, 2019, **45**(12), 14481–14489.
7 D. Jia, B. Liang, Z. Yang and Y. Zhou, *Prog. Mater. Sci.*, 2018, **98**, 1–67.
8 B. Matsoso, W. Hao, Y. Li, V. Vuillet-a-Ciles, V. Garnier, P. Steyer, B. Toury, C. Marichy and C. Journet, *J. Phys.: Mater.*, 2020, **3**, 034002.
9 K. Lin, X. Zong, P. Sheng, S. Zhao, Y. Qi, W. Zhang and S. Wu, *J. Eur. Ceram. Soc.*, 2023, **43**, 6804–6814.
10 A. H. Mir and S. N. Ahmad, *Proc. Inst. Mech. Eng., Part L*, 2021, **235**, 1739–1756.
11 R. Ji, Y. Liu, Y. Zhang and F. Wang, *Int. J. Refract. Met. Hard Mater.*, 2011, **29**, 117–122.
12 R. P. Chaudhary, C. Parameswaran, M. Idrees, A. S. Rasaki, C. Liu, Z. Chen and P. Colombo, *Prog. Mater. Sci.*, 2022, **128**, 100969.
13 F. W. Ainger and J. M. Herbert, *Angew. Chem., Int. Ed.*, 1959, **71**, 653.
14 P. Colombo, G. Mera, R. Riedel and G. D. Soraru, *J. Am. Ceram. Soc.*, 2010, **93**, 1805–1837.
15 S. Yajima, J. Hayashi, M. Omori and K. Okamura, *Nature*, 1976, **261**, 683–685.
16 F. Sarraf, S. V Churakov and F. Clemens, *Polymers*, 2023, **15**, 4360.
17 R. Riedel, A. Kienzle, W. Dressler, L. Ruwisch, J. Bill and F. Aldinger, *Nature*, 1996, **382**(6594), 796–798.
18 B. J. Ackley, K. L. Martin, T. S. Key, C. M. Clarkson, J. J. Bowen, N. D. Posey, J. F. Ponder Jr, Z. D. Apostolov, M. K. Cinibulk and T. L. Pruyn, *Chem. Rev.*, 2023, **123**, 4188–4236.
19 G. Mera and E. Ionescu, *Encyclopedia of Polymer Science and Technology*, 2002.
20 D. Eliche-Quesada, L. Pérez-Villarejo and P. J. Sánchez-Soto, *Ceramic Materials - Synthesis, Characterization, Applications and Recycling*, 2019.
21 R. N. Katz, *Materials and Mechanical Design*, 2006, p. 433.
22 R. Riedel, E. Ionescu and I. Chen, *Ceramics Science and Technology: Volume 1: Structures*, 2008, pp. 1–38.
23 V. Khabashesku, V. Filonenko, R. Bagramov, I. Zibrov and A. Anokhin, *ACS Appl. Mater. Interfaces*, 2021, **13**(49), 59560–59566.
24 O. Icin, D. Zeydanlı, M. Biesuz and G. D. Soraru, *Open Ceram.*, 2025, 100803.
25 Q. D. Nghiem, S. J. Cho and D.-P. Kim, *J. Mater. Chem.*, 2006, **16**, 558–562.
26 S. Zhou, L. Yao, T. Zhao, H. Mei, L. Cheng and L. Zhang, *Carbon*, 2022, **196**, 253–263.
27 M. Chen, R. Shang, P. M. Sberna, M. W. J. Luiten-Olieman, L. C. Rietveld and S. G. J. Heijman, *Sep. Purif. Technol.*, 2020, **253**, 117496.
28 Y. Jüttke, H. Richtera, I. Voigta, R. M. Prasadb, M. S. Bazarjanib, A. Gurlob and R. Riedelb, *Chem. Eng.*, 2013, **32**, 1891–1896.
29 A. H. Raza, S. Farhan, A. Ali, A. Sarfraz, M. A. Ahmad, M. Syväjärvi and R. Raza, *J. Solid State Electrochem.*, 2024, 1–9.
30 A. Samadi, L. Gao, L. Kong, Y. Orooji and S. Zhao, *Resour., Conserv. Recycl.*, 2022, **185**, 106497.
31 Y. Wang, X. Pei, H. Li, X. Xu, L. He, Z. Huang and Q. Huang, *Ceram. Int.*, 2020, **46**, 28300–28307.
32 K. Takeuchi, T. Suga and E. Higurashi, *Sci. Rep.*, 2024, **14**, 1267.
33 J. E. Mark, *Acc. Chem. Res.*, 2004, **37**, 946–953.
34 G. D. Sorarù, K. Girardini, M. Narisawa and M. Biesuz, *J. Am. Ceram. Soc.*, 2021, **104**, 3097–3104.
35 M. Pelanconi, S. Bottacin, P. Colombo and A. Ortona, *J. Eur. Ceram. Soc.*, 2023, **43**, 5871–5881.
36 K. Sokolowski, S. Blazewicz, M. M. Marzec, A. Bernasik and A. Fraczek-Szczypta, *Surf. Coat. Technol.*, 2024, **484**, 130804.
37 K. Yuan, D. Han, J. Liang, W. Zhao, M. Li, B. Zhao, W. Liu, H. Lu, H. Wang and H. Xu, *J. Adv. Ceram.*, 2021, **10**, 1140–1151.
38 Q. Chen, D. Jia, B. Liang, Z. Yang, Y. Zhou, D. Li, R. Riedel, T. Zhang and C. Gao, *Ceram. Int.*, 2021, **47**, 10958–10964.
39 G. S. Krishnan, T. Ramcharan, R. R. Rao and S. Naveen, *Ceram. Int.*, 2021, **47**, 17502–17509.
40 M. Arango-Ospina, F. Xie, I. Gonzalo-Juan, R. Riedel, E. Ionescu and A. R. Boccaccini, *Appl. Mater. Today*, 2020, **18**, 100482.
41 T. Centofanti, M. d. A. Silva, M. G. Segatelli and C. R. T. Tarley, in *Recent Advancements in Polymeric Materials for Electrochemical Energy Storage*, Springer, 2023, pp. 449–465.
42 C. Stabler, F. Roth, M. Narisawa, D. Schliephake, M. Heilmaier, S. Lauterbach, H.-J. Kleebe, R. Riedel and E. Ionescu, *J. Eur. Ceram. Soc.*, 2016, **36**, 3747–3753.
43 A. V Rau, K. Knott and K. Lu, *Mater. Chem. Front.*, 2021, **5**, 6530–6545.
44 X. Guo, H. Wang, N. Fu, P. Xing, S. Wang, B. Wu and Y. Zhuang, *Int. J. Appl. Ceram. Technol.*, 2024, **21**, 1372–1381.
45 E. Ionescu and R. Riedel, *Ceramics and composites processing methods*, 2012, pp. 235–270.
46 Z. Ren, S. Bin Mujib and G. Singh, *Materials*, 2021, **14**, 614.
47 L. J. Print, J. J. Liggat, S. Moug, H. Seaton and D. C. Apperley, *Silicon*, 2023, **15**, 1355–1379.
48 A. C. Pierre, *Introduction to sol-gel processing*, Springer Nature, 2020.

49 K. A. Yur'evich, D. F. Valer'evich, V. S. Ivanov, A. S. Yegorov and V. V. Men'shikov, *Orient. J. Chem.*, 2018, **34**, 612.
50 B. Arkles, *Chemical Industries*, Marcel Dekker, New York, 1996, pp. 667–676.
51 R. P. D'Amelia, J. Mancuso, W. F. Nirode and S. Singh, *World J. Org. Chem.*, 2019, **7**, 5–13.
52 S. C. Shit and P. Shah, *Natl. Acad. Sci. Lett.*, 2013, **36**, 355–365.
53 E. V. Egorova, N. G. Vasilenko, N. V. Demchenko, E. A. Tatarinova and A. M. Muzafarov, in *Doklady Chemistry*, Springer, 2009, vol. 424, pp. 15–18.
54 F. Sarraf, S. V. Churakov and F. Clemens, *Polymers*, 2023, **15**(22), 4360.
55 S. Beppu, Y. Tachibana and K. I. Kasuya, *MRS Online Proc. Libr.*, 2023, **12**(4), 536–542.
56 S. Fu, M. Zhu and Y. Zhu, *J. Adv. Ceram.*, 2019, **8**, 457–478.
57 C. Chen, Z. Luo, H. Zeng, C. Hao, K.-F. Yang, Z. Li, G.-Q. Lai and P. Zhang, *Macromolecules*, 2024, **57**, 8146–8153.
58 M. Gerwig, U. Böhme and M. Friebel, *Chem.–Eur. J.*, 2024, e202400013.
59 S. K. Shukla, R. K. Tiwari, A. Ranjan, A. K. Saxena and G. N. Mathur, *Thermochim. Acta*, 2004, **424**, 209–217.
60 C. Vakifahmetoglu, I. Menapace, A. Hirsch, L. Biasetto, R. Hauser, R. Riedel and P. Colombo, *Ceram. Int.*, 2009, **35**, 3281–3290.
61 C. W. Chen, C. C. Huang, Y. Y. Lin, L. C. Chen and K. H. Chen, *Diamond and Related Materials*, 2005, **14**, 1126–1130.
62 J. F. Wendel, N. Matthée, S. Schafföner and G. Motz, *J. Am. Ceram. Soc.*, 2025, e20634.
63 A. V Barysheva, G. M. Mochalov and S. S. Suvorov, *Russ. J. Appl. Chem.*, 2021, **94**, 1226–1231.
64 C. Racles, M. Dascalu, A. Bele and M. Cazacu, *Reactive and Functional Polymers Volume One: Biopolymers, Polyesters, Polyurethanes, Resins and Silicones*, 2020, pp. 235–291.
65 F. Hosseini, K. J. Fadaee, Z. Salari and M. Ebrahimi, *Chem. Methodol.*, 2023, **7**(5), 383–391.
66 J. L. Jayanthi, R. Palavalasa, S. Jampani, V. Miditana and G. Jalem, *Chem. Methodol.*, 2023, **7**(7), 569–580.
67 A. Abd Al Zahra and A. K. M. A. Al Sammarraie, *Chem. Methodol.*, 2022, **6**(1), 67–73.
68 D. Erb and K. Lu, *Microporous Mesoporous Mater.*, 2018, **266**, 75–82.
69 S. J. Widgeon, *Spectroscopic and calorimetric investigation of short and intermediate-range structures and energetics of amorphous SiCO, SiCN, and SiBCN polymer-derived ceramics*, University of California, Davis, 2013.
70 M. Weinmann, *Chemical Processing of Ceramics*, 2005, p. 439.
71 H. Zhang, L. Xue, J. Li and Q. Ma, *Polymers*, 2020, **12**, 672.
72 S. Widgeon, G. Mera, Y. Gao, S. Sen, A. Navrotsky and R. Riedel, *J. Am. Ceram. Soc.*, 2013, **96**, 1651–1659.
73 R. D. Archer, *Inorganic and organometallic polymers*, John Wiley & Sons, 2004.
74 J. Yuan and A. H. E. Müller, *Polymer*, 2010, **51**, 4015–4036.
75 S. Mazerat and R. Pailler, *Ceram. Int.*, 2021, **47**, 2888–2891.
76 H. G. Hackbarth, T. S. Key, B. J. Ackley, G. Opletal, A. Rawal, L. Gallington, Y. Yang, L. Thomsen, M. B. Dickerson and T. L. Pruyn, *J. Eur. Ceram. Soc.*, 2024, **44**, 1932–1945.
77 Q. Wang, L. Yu, H. Nagasawa, M. Kanezashi and T. Tsuru, *Sep. Purif. Technol.*, 2020, **248**, 117067.
78 A. Xia, J. Yin, X. Chen, X. Liu and Z. Huang, *Crystals*, 2020, **10**, 824.
79 M. A. Mazo, A. C. Caballero and J. Rubio, *J. Alloys Compd.*, 2021, **889**, 161698.
80 G. Pang, F. Meng, Y. Chen, A. Katre, J. Carrete, B. Dongre, G. K. H. Madsen, N. Mingo and W. Li, *Mater. Today Phys.*, 2024, **41**, 101346.
81 B. Santhosh, C. Vakifahmetoglu, E. Ionescu, A. Reitz, B. Albert and G. D. Soraru, *Ceram. Int.*, 2020, **46**, 5594–5601.
82 H. Ramlow, L. F. B. Ribeiro, S. Schafföner, G. Motz and R. A. F. Machado, *J. Eur. Ceram. Soc.*, 2024, **44**, 5308–5318.
83 M. Balestrat, E. D. Acosta, O. Hanzel, N. Tessier-Doyen, R. Machado, P. Šajgalík, Z. Lenčéš and S. Bernard, *J. Eur. Ceram. Soc.*, 2020, **40**, 2604–2612.
84 P. Wang, F. Liu, H. Wang, H. Li and Y. Gou, *J. Mater. Sci. Technol.*, 2019, **35**(12), 2743–2750.
85 A. Xia, J. Yin, X. Chen, X. Liu and Z. Huang, *Crystals*, 2020, **10**(9), 824.
86 L. C. Pardini and M. L. Gregori, *J. Aerosp. Technol. Manage.*, 2010, **2**(2), 183–194.
87 R. Sujith, S. Jothi, A. Zimmermann, F. Aldinger and R. Kumar, *Int. Mater. Rev.*, 2021, **66**, 426–449.
88 S. Yajima, T. Iwai, T. Yamamura, K. Okamura and Y. Hasegawa, *J. Mater. Sci.*, 1981, **16**, 1349–1355.
89 T. Ishikawa, Y. Kohtoku, K. Kumagawa, T. Yamamura and T. Nagasawa, *Nature*, 1998, **391**, 773–775.
90 J. Liu, Z. Ahmad and J. Chen, *Ceram. Int.*, 2024, **50**, 16284–16291.
91 M. A. Mazo, D. Soriano and J. Rubio, *Ceram. Int.*, 2023, **49**, 12866–12875.
92 Q. Hanniet, E. Petit, S. Calas-Etienne, P. Etienne, K. Aissou, C. Gervais, P. Miele, B. Charlot and C. Salameh, *Mater. Des.*, 2022, **223**, 111234.
93 T. Rouxel, J. Sanglebœuf, J. Guin, V. Keryvin and G. Soraru, *J. Am. Ceram. Soc.*, 2001, **84**, 2220–2224.
94 S. Walter, G. D. Soraru, H. Brequel and S. Enzo, *J. Eur. Ceram. Soc.*, 2002, **22**, 2389–2400.
95 G. D. Sorarù, L. Kundanati, B. Santhosh and N. Pugno, *J. Am. Ceram. Soc.*, 2019, **102**, 907–913.
96 N. Janakiraman, Z. Burghard and F. Aldinger, *J. Non-Cryst. Solids*, 2009, **355**, 2102–2113.
97 A. Bauer, M. Christ, A. Zimmermann and F. Aldinger, *J. Am. Ceram. Soc.*, 2001, **84**, 2203–2207.
98 T. Noda, *Handbook of Advanced Ceramics and Composites*, 2019, pp. 1–26.
99 Y. Katsuda, P. Gerstel, J. Narayanan, J. Bill and F. Aldinger, *J. Eur. Ceram. Soc.*, 2006, **26**, 3399–3405.
100 S. Bernard, D. Cornu, P. Miele, M. Weinmann and F. Aldinger, *Mechanical Properties and Performance of Engineering Ceramics and Composites: Ceramic Engineering and Science Proceedings*, 2005, vol. 26, pp. 35–42.
101 G. Chollon, *J. Eur. Ceram. Soc.*, 2000, **20**, 1959–1974.

102 G. Chollon, *Polymer Derived Ceramics: From Nano-structure to Applications*, 2010, pp. 292–308.
103 A. Kovalčíková, J. Sedláček, Z. Lenčéš, R. Bystrický, J. Dusza and P. Šajgalík, *J. Eur. Ceram. Soc.*, 2016, **36**, 3783–3793.
104 G. J. Leonel, X. Guo, G. Singh, C. Gervais and A. Navrotsky, *J. Am. Ceram. Soc.*, 2023, **106**, 5086–5101.
105 R. Michelle Morcos, G. Mera, A. Navrotsky, T. Varga, R. Riedel, F. Poli and K. Müller, *J. Am. Ceram. Soc.*, 2008, **91**, 3349–3354.
106 E. Butchereit and K. G. Nickel, *J. Mater. Process. Manuf. Sci.*, 1998, 15–21.
107 K. G. Nickel, E. Butchereit and C. Schumacher, *On the Role of Boron in the Oxidation of Si-CNB Ceramics*, The Electrochemical Society, 2000, p. 365.
108 Y. Wang, Y. Fan, L. Zhang, W. Zhang and L. An, *Scr. Mater.*, 2006, **55**, 295–297.
109 G. D. Sorarù, S. Modena, E. Guadagnino, P. Colombo, J. Egan and C. Pantano, *J. Am. Ceram. Soc.*, 2002, **85**, 1529–1536.
110 R. G. Jones and S. J. Holder, *Silicon-Containing Polymers: The Science and Technology of Their Synthesis and Applications*, 2000, pp. 353–373.
111 M. Parchovianský, I. Parchovianská, P. Švančárek, D. Medveď, M. Lenz-Leite, G. Motz and D. Galusek, *Molecules*, 2021, **26**, 2388.
112 G. Mera, M. Gallei, S. Bernard and E. Ionescu, *Nanomaterials*, 2013, **5**(2), 468–540.
113 F. Li, L. Zhou, J.-X. Liu and G.-J. Zhang, *Materials*, 2022, **16**, 220.
114 D. Erb and K. Lu, *J. Eur. Ceram. Soc.*, 2017, **37**, 4547–4557.
115 E. Bernardo, L. Fiocco, G. Parcianello, E. Storti and P. Colombo, *Materials*, 2014, **7**(3), 1927–1956.
116 G. Hasegawa, K. Kanamori, K. Nakanishi and T. Hanada, *J. Mater. Chem.*, 2009, **19**, 7716–7720.
117 C. Durif, M. Wynn, M. Balestrat, G. Franchin, Y.-W. Kim, A. Leriche, P. Miele, P. Colombo and S. Bernard, *J. Eur. Ceram. Soc.*, 2019, **39**, 5114–5122.
118 J. Gu, S. H. Lee, H. S. Lee and J. S. Kim, *J. Eur. Ceram. Soc.*, 2021, **41**(4), 2297–2305.
119 B. J. Ackley, K. L. Martin, T. S. Key, C. M. Clarkson, J. J. Bowen, N. D. Posey, J. F. Ponder Jr, Z. D. Apostolov, M. K. Cinibulk, T. L. Pruyn and M. B. Dickerson, *Chem. Rev.*, 2023, **123**(8), 4188–4236.
120 Z. Yu, N. Yang, V. Apostolopoulou-Kalkavoura, B. Qin, Z. Ma, W. Xing, C. Qiao, L. Bergström, M. Antonietti and S. Yu, *Angew. Chem., Int. Ed.*, 2018, **57**, 4538–4542.
121 A. Feinle, M. S. Elsaesser and N. Huesing, *Chem. Soc. Rev.*, 2016, **45**, 3377–3399.
122 H. Shi, J. Yang, Z. Li and C. He, *Silicon Containing Hybrid Copolymers*, 2020, pp. 1–21.
123 H. Shi, J. Yang, Z. Li and C. He, *Silicon Containing Hybrid Copolymers*, 2020, pp. 1–21.
124 P. Zhang, J. Duan, G. Chen, J. Li and W. Wang, *Sol. Energy*, 2018, **175**, 44–53.
125 H. Chaney and K. Lu, *Chem. Mater.*, 2023, **35**, 3902–3910.
126 S. Sun, J. Yuan, W. Guo, X. Duan, D. Jia and H. Lin, *J. Am. Ceram. Soc.*, 2024, **107**, 777–784.
127 A. Baux, A. Goillot, S. Jacques, C. Heisel, D. Rochais, L. Charpentier, P. David, T. Piquero, T. Chartier and G. Chollon, *J. Eur. Ceram. Soc.*, 2020, **40**, 2834–2854.
128 Y. Jia, T. D. Ajayi, M. A. Roberts Jr, C.-C. Chung and C. Xu, *ACS Appl. Mater. Interfaces*, 2020, **12**, 46254–46266.
129 Z. Cui, X. Chen, X. Li and G. Sui, *Sens. Actuators, A*, 2023, **350**, 114144.
130 Y. J. Joo and K. Y. Cho, *Mater. Res. Express*, 2021, **8**, 035603.
131 Y. Jia, M. A. R. Chowdhury, D. Zhang and C. Xu, *ACS Appl. Mater. Interfaces*, 2019, **11**, 45862–45874.
132 B. H. Costa, C. R. T. Tarley, E. S. Ribeiro and M. G. Segatelli, *Process. Appl. Ceram.*, 2023, **17**, 118–132.
133 A. Francis, R. Detsch and A. R. Boccaccini, *Ceram. Int.*, 2016, **42**, 15442–15448.
134 A. Nyczyk-Malinowska, W. Niemiec, G. Smoła, R. Gaweł, M. Szuwarzyński and Z. Grzesik, *Surf. Coat. Technol.*, 2021, **407**, 126760.
135 C. Linck, E. Ionescu, B. Papendorf, D. Galuskova, D. Galusek, P. Ŝajgalík and R. Riedel, *Int. J. Mater. Res.*, 2012, **103**, 31–39.
136 M. Nastasi, Q. Su, L. Price, J. A. C. Santana, T. Chen, R. Balerio and L. Shao, *J. Nucl. Mater.*, 2015, **461**, 200–205.
137 P. Colombo, T. E. Paulson and C. G. Pantano, *J. Sol-Gel Sci. Technol.*, 1994, **2**, 601–604.
138 K. Wang, M. Günthner, G. Motz and R. K. Bordia, *J. Eur. Ceram. Soc.*, 2011, **31**, 3011–3020.
139 W. Niemiec, P. Szczygieł, P. Jeleń and M. Handke, *J. Mol. Struct.*, 2018, **1164**, 217–226.
140 J. Bill and D. Heimann, *J. Eur. Ceram. Soc.*, 1996, **16**, 1115–1120.
141 B. Liu, J. Sun, L. Guo, H. Shi, G. Feng, L. Feldmann, X. Yin, R. Riedel, Q. Fu and H. Li, *Mater. Sci. Eng., R*, 2025, **163**, 100936.
142 G. S. Barroso, W. Krenkel and G. Motz, *J. Eur. Ceram. Soc.*, 2015, **35**, 3339–3348.
143 F. Niu, Y. Wang, I. Abbas, S. Fu and C. Wang, *Ceram. Int.*, 2017, **43**, 3238–3245.
144 M. C. Bruzzoniti, M. Appendini, B. Onida, M. Castiglioni, M. Del Bubba, L. Vanzetti, P. Jana, G. D. Sorarù and L. Rivoira, *Environ. Sci. Pollut. Res.*, 2018, **25**, 10619–10629.
145 T. Xu, R. Qu, Y. Zhang, C. Sun, Y. Wang, X. Kong, X. Geng and C. Ji, *Frontiers in Environmental Chemistry*, 2021, **2**, 706254.
146 M. C. Bruzzoniti, M. Appendini, L. Rivoira, B. Onida, M. Del Bubba, P. Jana and G. D. Sorarù, *J. Am. Ceram. Soc.*, 2018, **101**, 821–830.
147 J. Pan, J. Ren, Y. Xie, X. Wei, Y. Guan, X. Yan, H. Tang and X. Cheng, *Res. Chem. Intermed.*, 2017, **43**, 3813–3832.
148 J. Pan, W. Shen, Y. Zhao, H. Sun, T. Guo, Y. Cheng, N. Zhao, H. Tang and X. Yan, *Colloids Surf., A*, 2020, **584**, 124041.
149 D. Zeydanli, S. Akman and C. Vakifahmetoglu, *J. Am. Ceram. Soc.*, 2018, **101**, 2258–2265.
150 G. Pezzotti, *J. Ceram. Soc. Jpn.*, 2023, **131**, 398–428.
151 G. Sharma, A. Kumar, S. Sharma, M. Naushad, P. Dhiman, D.-V. N. Vo and F. J. Stadler, *Mater. Lett.*, 2020, **278**, 128359.
152 Y. Niu, R. Qu, X. Liu, L. Mu, B. Bu, Y. Sun, H. Chen, Y. Meng, L. Meng and L. Cheng, *Mater. Res. Bull.*, 2014, **52**, 134–142.

153 Y. Wang, R. Qu, F. Pan, X. Jia, C. Sun, C. Ji, Y. Zhang, K. An and Y. Mu, *Chem. Eng. J.*, 2017, **317**, 187–203.
154 C. Moysan, R. Riedel, R. Harshe, T. Rouxel and F. Augereau, *J. Eur. Ceram. Soc.*, 2007, **27**, 397–403.
155 K. Lu, D. Erb and M. Liu, *J. Mater. Chem. C*, 2016, **4**, 1829–1837.
156 Y. Wang, X. Guo, Y. Feng, X. Lin and H. Gong, *Ceram. Int.*, 2017, **43**, 15551–15555.
157 Y. Liu, Y. Feng, H. Gong, Y. Zhang, X. Lin, B. Xie and J. Mao, *J. Alloys Compd.*, 2018, **749**, 620–627.
158 Y. Hou, L. Cheng, Y. Zhang, Y. Yang, C. Deng, Z. Yang, Q. Chen, X. Du and L. Zheng, *ACS Appl. Mater. Interfaces*, 2017, **9**, 43072–43080.
159 Y. Feng, X. Guo, J. Lu, J. Liu, G. Wang and H. Gong, *Ceram. Int.*, 2021, **47**, 19582–19594.
160 X. Guo, J. Lu, J. Liu, C. Liu, Y. Tong, J. Li, H. Sun, H. Peng, S. Wu and Y. Feng, *Ceram. Int.*, 2022, **48**, 20495–20505.
161 P. Wang, L. Cheng, Y. Zhang and L. Zhang, *ACS Appl. Mater. Interfaces*, 2017, **9**, 28844–28858.
162 P. Wang, L. Cheng and L. Zhang, *Carbon*, 2017, **125**, 207–220.
163 P. Wang, L. Cheng, Y. Zhang, W. Yuan, H. Pan and H. Wu, *Composites, Part A*, 2018, **104**, 68–80.
164 H. Ramlow, L. L. Silva, C. Marangoni, M. R. Baldan and R. A. F. Machado, *Diamond and Related Materials*, 2024, **144**, 110985.
165 W. Zhu, Z. Chen, J. Liang and D. Su, *Carbon*, 2022, **197**, 65–75.
166 Y. Song, S. Jin, K. Hu, Y. Du, J. Liang and J. Kong, *J. Am. Ceram. Soc.*, 2021, **104**, 5244–5256.
167 C. Luo, Y. Wang, X. Hu, Y. Wu, Y. Wang, M. Chao and L. Yan, *Mater. Res. Bull.*, 2024, **174**, 112718.
168 N. R. Nagaiah, J. S. Kapat, L. An and L. Chow, *J. Phys.: Conf. Ser.*, 2006, **34**, 458.
169 N. Li, Y. Cao, R. Zhao, Y. Xu and L. An, *Sens. Actuators, A*, 2017, **263**, 174–178.
170 M. Yang, C. Ma, Y. Hu, K. Wang, R. Zhao, Y. Liang, D. Han, H. Wang, R. Zhang and G. Shao, *Adv. Funct. Mater.*, 2024, 2400400.
171 Z. Yu, S. Li, P. Zhang, Y. Feng and X. Liu, *Ceram. Int.*, 2017, **43**, 4520–4526.
172 A. Javed, M. Islam, Y. O. Al-Ghamdi, M. Iqbal, M. Aljohani, S. Sohni, S. S. A. Shah and S. A. Khan, *Int. J. Biol. Macromol.*, 2024, **256**, 128363.
173 M. T. Genc, A. Sarilmaz, E. Aslan, F. Ozel and I. H. Patir, *Mol. Catal.*, 2024, **556**, 113915.
174 J. Essmeister, L. Schachtner, E. Szoldatits, S. Schwarz, A. Lichtenegger, B. Baumann, K. Föttinger and T. Konegger, *Open Ceram.*, 2023, **14**, 100350.
175 Z. Xu, J. Lu, G. Zhang, R. Liu, W. Zhang and Q. Meng, *Ceram. Int.*, 2024, **50**, 23115–23123.
176 N. Yu, Y. Wang, H. Cao, R. Si, Z. Xu, X. Hong, X. Mao, K. Shen and J. Wu, *Chem. Eng. J.*, 2024, **490**, 151851.
177 J. Jing, Y. Zhao, A. Saleam, H. Gong, Y. Zhang, M. Sheng and J. Lu, *J. Mater. Sci.: Mater. Electron.*, 2023, **34**, 1384.
178 X. Ji, R. Qiao, Z. Xu, J. Liu and H. Yuan, *Phys. Status Solidi A*, 2024, **221**, 2400121.
179 Q. Wang, Y. Peng, W. Jiang, H. Xu, W. Hai, Q. Shao and A. Li, *Ceram. Int.*, 2024, **50**, 20167–20175.
180 X. Lin, H. Gong and Z. Chen, *Ceram. Int.*, 2023, **49**, 23851–23863.
181 Q. Yan, S. Chen, H. Shi, X. Wang, S. Meng and J. Li, *J. Eur. Ceram. Soc.*, 2023, **43**, 7373–7380.
182 H. Wang, Z. Chen and D. Su, *J. Mater. Sci. Technol.*, 2024, **179**, 145–154.
183 A. Arora, P. Chander, S. Mourya, S. Singh, R. Chandra and V. K. Malik, *Appl. Surf. Sci.*, 2024, **665**, 160292.